Marià Montoro Bori

Battery Pack Design and Cell Tests for 48V EV

Treball Fi de Màster
dirigit pel Dr. Carlos Olalla Martínez

Màster en Tecnologies del Vehicle Elèctric

UNIVERSITAT ROVIRA I VIRGILI

Tarragona
2023

Contents table

Table of figures

1 Introduction

Around the year 2000, some car manufacturers like Toyota and Honda started selling electrified vehicles with the aim of offering highly efficient vehicles. Models like the Toyota Prius rapidly became a success due to its smooth driving and excellent fuel consumption in urban areas.

Figure 1: Toyota Prius' first generation

The demand for this type of vehicles kept increasing up to a point where nowadays, main car manufacturers worldwide sell electrified vehicles. In addition to that, the focus on climate change and the fact that big cities started to have significant pollution issues due to road traffic further increased the need for cleaner vehicles. Because of these reasons, battery electric vehicles (BEVs) started to be developed and sold quite early in the 21st century. The chart below shows the evolution of electrified vehicles in the US as an example:

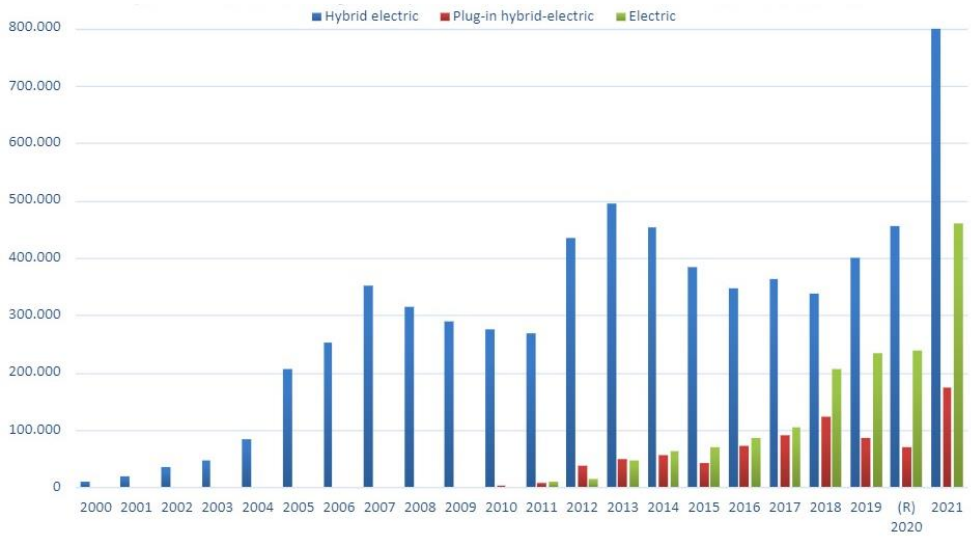

Figure 2: Electrified vehicle sales' evolution at the US [1]

The rise of BEVs pushed the industry to invest large amounts of resources in Battery technology in order to increase energy density of battery packs so BEVs had a bigger range (see chart below). All this battery pack/cell development has also brought the opportunity for other markets to move away from Internal Combustion Engines (ICE) and start selling electrified versions of their products.

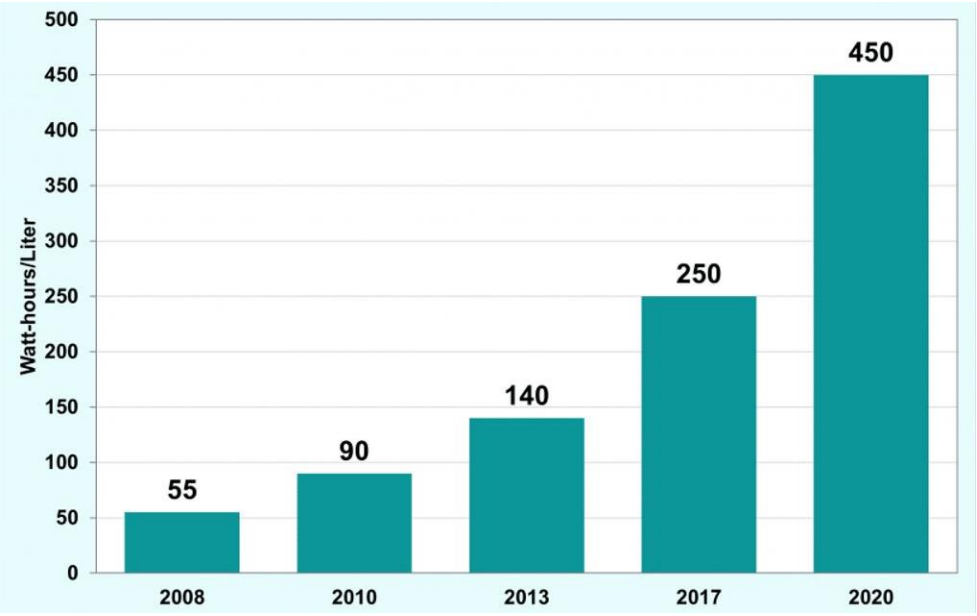

Figure 3: Energy Density evolution of Li-Ion Battery Packs between 2008 and 2020 [8]

Hence, nowadays we can see vehicles like excavators, recreational boats or tractors with an electric powertrain rather than combustion engines.

Whether Hybrid, Plug-In Hybrid or Pure Electric, new electrified vehicles contribute to the decarbonisation of our economy and have additional benefits like smooth and silent operation as well as a significantly lower maintenance cost. Specially if the Electricity mix is mostly dominated by Renewable Energies, EVs become clear winners when it comes to reduce lifetime emissions. [10]

Image below shows that even in Poland, where the electricity mix is not favourable due to the large use of Coal power plants to generate electricity, EV lifetime emissions are already better than Petrol/Diesel alternatives:

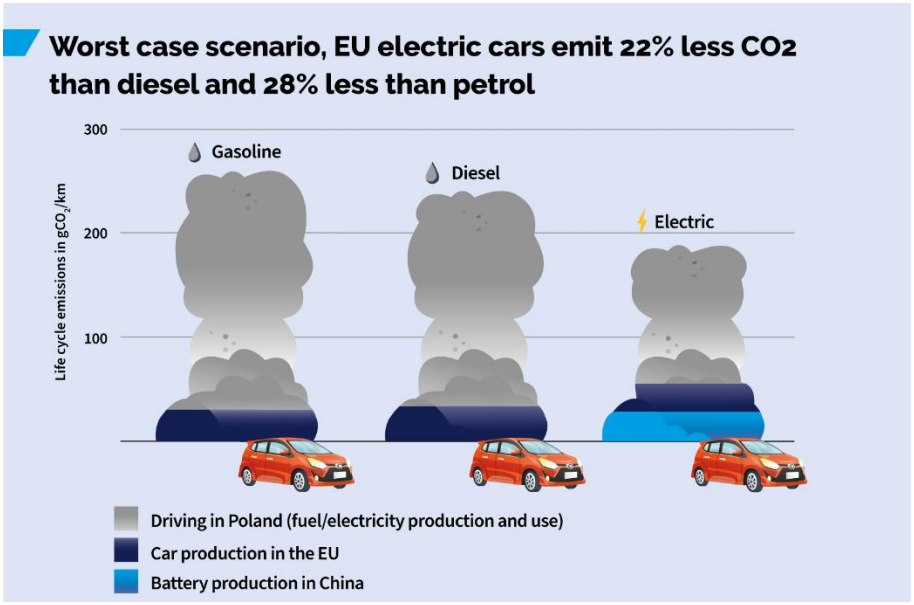

Figure 4: Life cycle emissions at worst case scenario (low clean energy development). [9]

Furthermore, the situation gets much better when countries with strong renewable energy sources are reviewed:

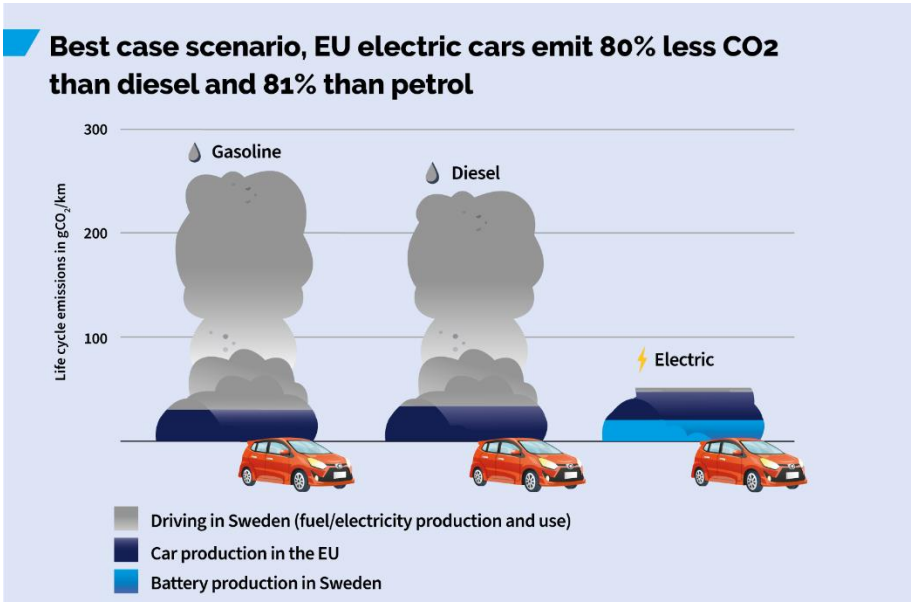

Figure 5: Life cycle emissions at best case scenario (high clean energy development). [9]

Furthermore, some car manufacturers like Volvo have performed their own studies to analyse the lifetime emissions of BEVs and the outcome has also been that lifetime emissions are lower compared to petrol/diesel competitors:

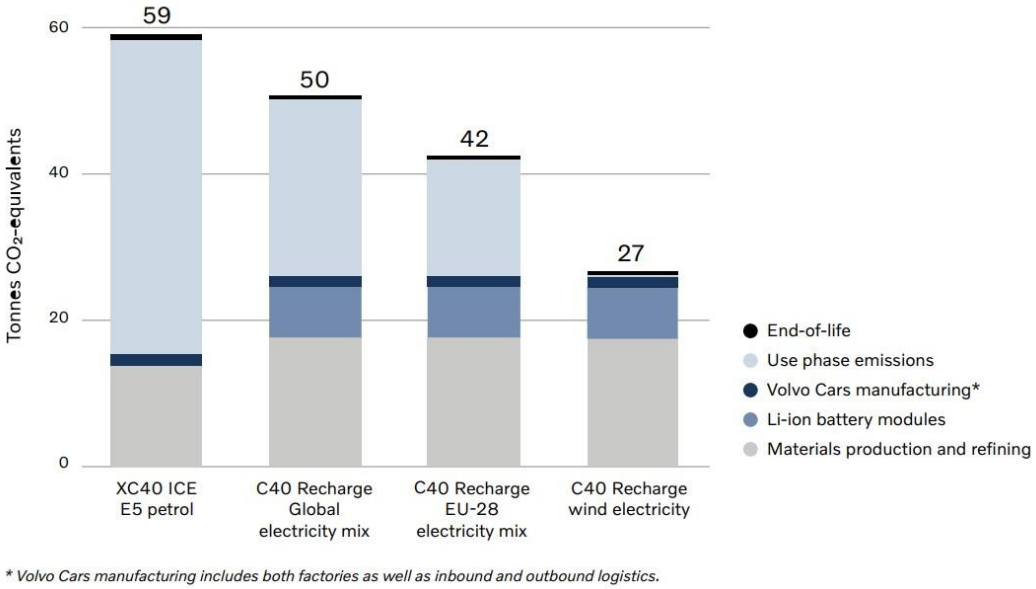

Figure 6: Volvo owned study in which life cycle emissions are compared too.[12]

Another type of vehicle which is also seeing this trend is Karts. Whether for racing or recreational use, electric karts (also called eKarts) are already being sold by some important Kart manufacturers worldwide. One of the main Kart manufacturers in Spain is "BRB Karts", which is a Kart manufacturer located in Tarragona Area. This company is already selling eKarts successfully but on the other hand, it is also looking at ways of reducing the price of its eKarts while maintaining a good level of performance and obviously safety.

The work carried out during this Dissertation pursues the target of finding out whether some specific Cell chemistry would be able to perform sufficiently well while having a lower cost than the actual technology being used at BRB Karts.

2 Cell performance targets

One of the aims of this Project is to prove whether a specific cell type and chemistry are suitable for an eKart application. An eKart requires a Battery Pack of a contained size, mainly because the chassis of the vehicle does not offer a lot of packaging space.

Weight is also a factor to take into account as in the end, an eKart is designed to be fast and to have good handling capabilities so it is fun to drive. On the other hand, it is important to remember that an eKart designed for rental purposes does not require ultimate performance but mainly high reliability while having a decent performance.

For reference, the specs of the BRB AM2´s eKart Battery Pack are shown below:

	Weight (kg)	Length (mm)	Width (mm)	Height (mm)	Approx. Volume (L)	Capacity (kWh)
BRB's AM2 eKart Battery Pack	25	590	200	290	34.22	4.3

The current pack is made with cylindrical Li-Ion cells of undeclared chemistry and size, although they are suspected to be either 18650 or 21700 type Cells. As shown below, Li-Ion technology offers a higher overall performance compared to other chemistries like AGM, Lead-Acid or Ni-Mh.[2] This is why it is used in most electric vehicle applications.[5] For this reason, in this Project only Li-Ion chemistries have been considered. The chart below shows how Li-Ion technology is clearly a winner in terms of volumetric and specific energy density:

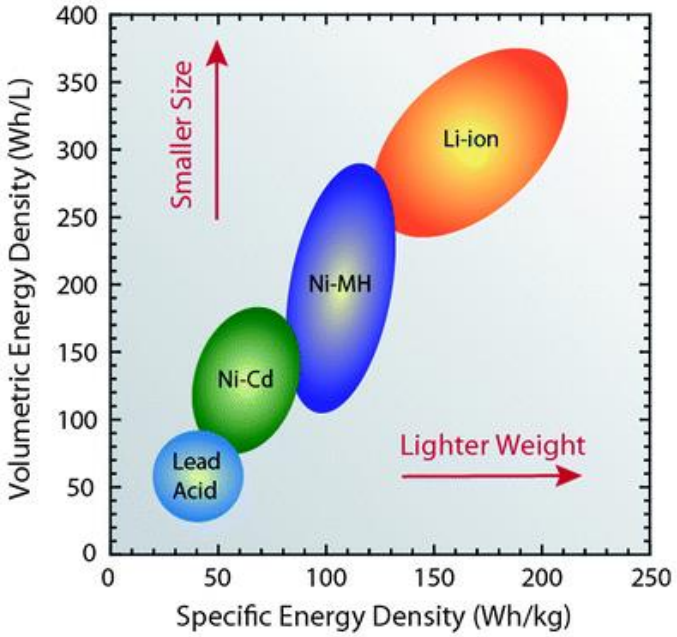

Figure 7: Volumetric and Specific Energy Density comparison of different Cell types.[2]

When it comes to electric vehicle applications, cylindrical cells are widely used within the industry. A photo of a Tesla battery pack is shown below:

Figure 8: Tesla Model 3 battery section [11]

Cylindrical cells can have different sizes but 18650 and 21700 types are two of the most common sizes. The table below shows how many cells (and their configuration) would be needed to obtain similar voltage and capacity figures as the current AM2 eKart:

	Cell Voltage (V)	Cell capacity (Ah)	Number of Series connected Cells	Number of Parallel connected Cells	Total number of Cells	Cell Weight (kg)	Total Cell Weight (kg)
"Generic" LFP 18650	3.2	1.8	15	50	750	0.042	31.5
LG 18650	3.65	2.6	13	34	442	0.044	19.5
SANYO NCR20700A	3.6	3.3	14	28	392	0.063	24.7
SAMSUNG 40T 21700	3.6	4	13	22	286	0.07	20

In the case of either 18650 or 21700 Cells, it can be seen that at least around 300 cells are necessary to obtain the required capacity. Although this is possible, having so many cells means there are many more connections that can fail and in addition, the complexity and time to manufacture is significantly higher. This fact obviously impacts the final price of the pack, which at this moment is very high.

Apart from cylindrical cells, prismatic cells are another option. This type of cell is commonly used with the Lithium-Iron-Phosphate (LFP) chemistry. An example of some LFP prismatic cells can be seen below:

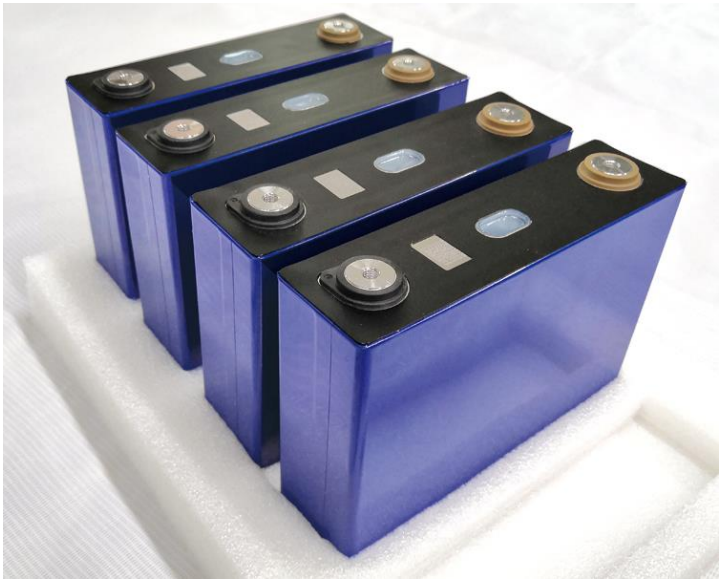

Figure 9: Example of Li-ion prismatic LFP cells.[4]

This type of cell has some advantages compared to smaller cylindrical cells [2][8]:

- Higher capacity per cell (much less cells needed per Pack).
- Very good life cycle.
- Less connections within pack, offering higher reliability.
- Lower manufacturing cost.

Regarding the disadvantages [2][8]:

- Lower energy density than cylindrical cells (in the case of LFP cells).
- Higher weight and volume to obtain same power/capacity.
- Lower peak charge/discharge power.
- Potential worse cooling efficiency.

Looking at the different advantages and disadvantages, prismatic cells may be a good option for applications in which high power and low weight are not a top priority. Additionally, in the case of LFP Prismatic cells, they offer great safety (no thermal runaway) and are a more environmentally friendly option compared to chemistries like NCA (Nickel/Cobalt/Aluminium) or NMC (Nickel/Manganese/Cobalt). These chemistries contain Cobalt, which is a mineral linked to child labour and worker exploitation in some African countries, mainly in the Democratic Republic of the Congo. [14]

These are the main reasons why car manufacturers are slowly increasing the use of LFP cells on their vehicles. Manufacturers like Tesla, BYD or Nissan are already using this chemistry for some of their cars. [7]

Because of the above, prismatic LFP cells have been chosen as the technology which could allow the built of a pack that would give the needed performance at a reasonable price.

3 Load applied to cells

One of the aims of this project is to simulate how an LFP battery pack would behave if it was to be used on a light vehicle application like an eKart. To accomplish this, the following steps have been completed in order to obtain a current profile which can be used on an electronic load and therefore discharge cells as if they were in an eKart.

3.1 Karting Circuit Speed Profile

The first step has been to obtain a speed profile of a Karting circuit so a real application is represented. In this case, the circuit chosen has been the one below:

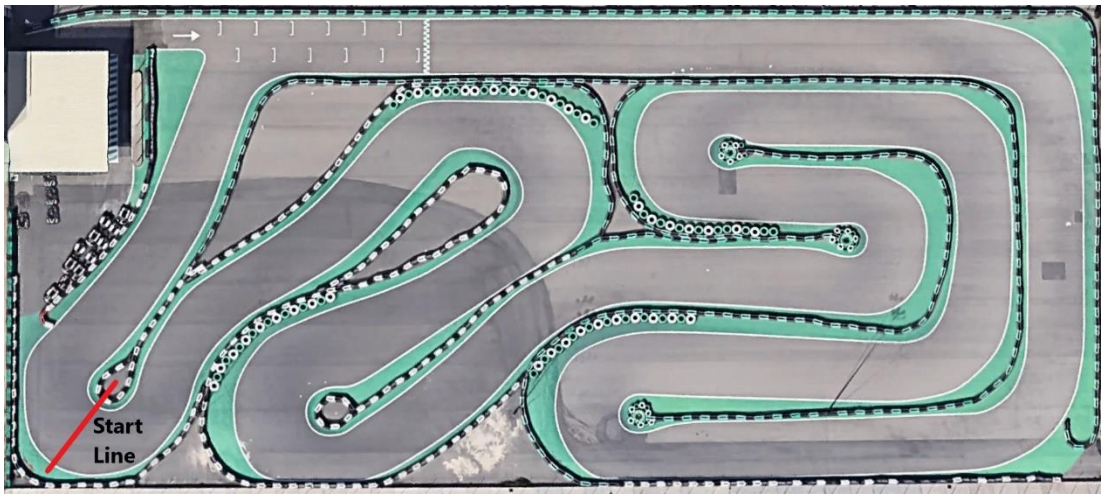

Figure 10: Karting Circuit map

Several laps have been completed using an electric kart equipped with a GPS logger. Considering the speed can be obtained by deriving position data over time, a speed profile of one lap has been obtained:

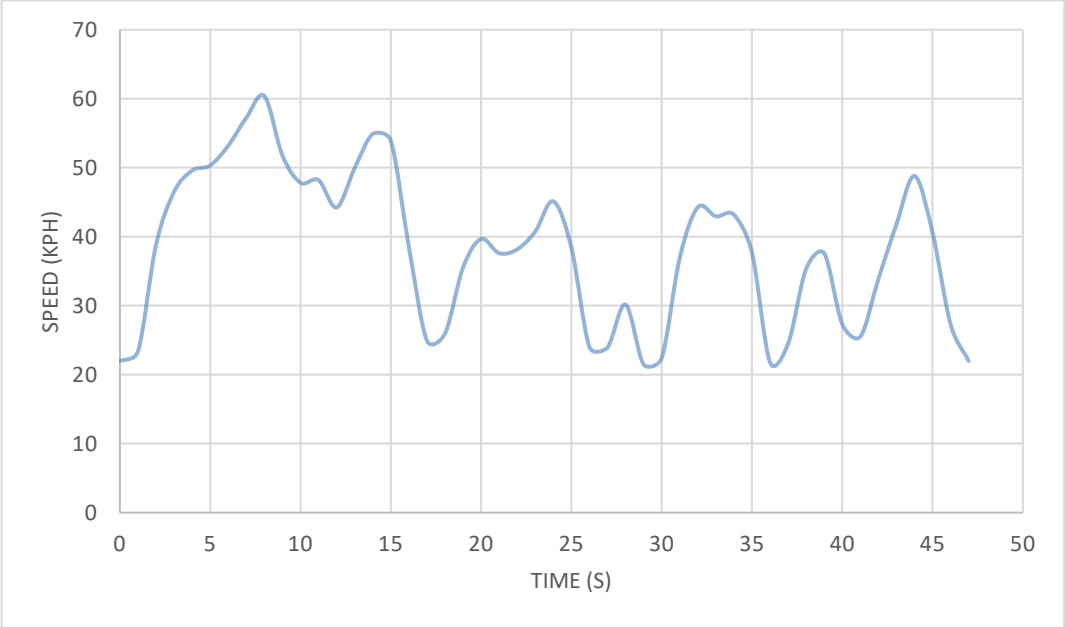

Figure 11: One Lap Speed Profile

3.2 Power Profile

Once a realistic speed profile is obtained, the next step is to work out what the power profile would be considering the physical parameters of the e-Kart. A Simulink model is used for this purpose. The Simulink model is originally from the "Energy Storage Systems" subject from the URV´s Master of Electric Vehicle Technology. The model has been modified in order to take in the GPS data from the Karting Circuit and to account for specific eKart parameters. This model is shown below:

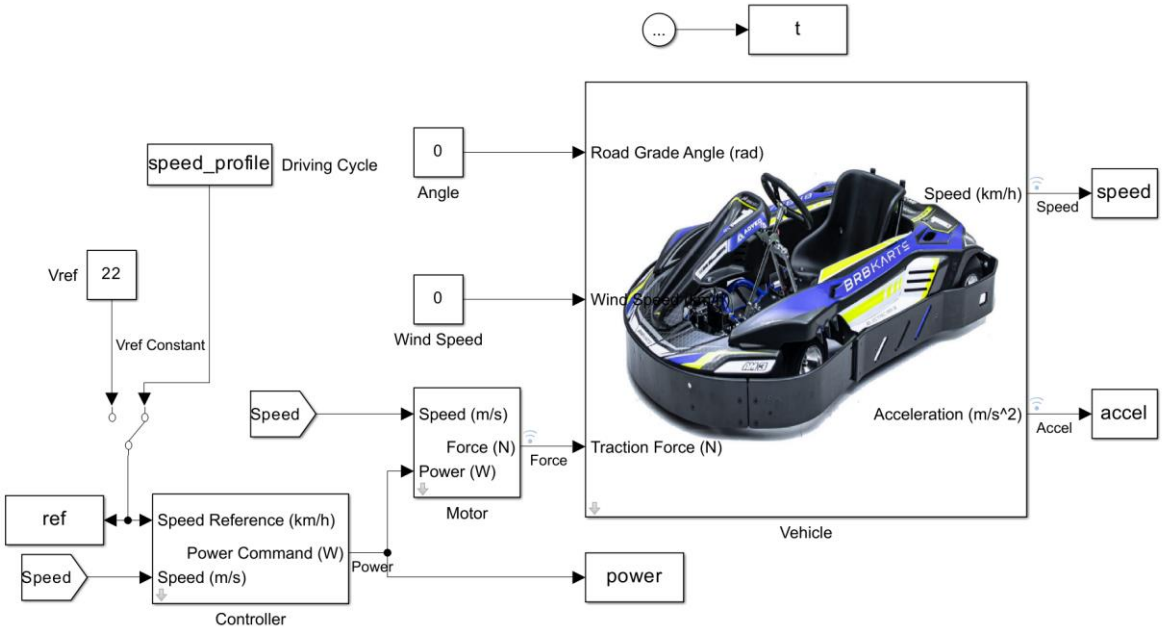

Figure 12: Simulink model

On the model above, a "Vehicle" block has some inputs in order to represent the real vehicle specifications:

eKart parameters	
Weight (with driver)	230 kg
Rolling coefficient	0.03
Drag coefficient	0.6

Additionally, the "Vehicle" block can also consider wind speed and road grade to calculate braking forces but in this case, both have been deemed negligible. This is because the day the GPS data was logged, wind speed was really low and also because that Track has no significant inclination.

The "speed profile" block is essentially the speed profile of the track which has been presented previously.

From the speed profile and the vehicle data, the model is able to calculate how much power is needed to complete a lap as per the recorded GPS data.

A brief description of the mathematics used in the model is presented below:

Newton's second law of motion:

$$F = m \times a \tag{1}$$

Where:

F: Force that moves a body (N)

m: Mass of the body (kg)

a: Body's acceleration (m/s^2)

Same expression but applied to a vehicle in motion is shown below:

$$\frac{dV}{dt} = \frac{\sum F_t - \sum F_b}{m} \tag{2}$$

In this case:

$\frac{dV}{dt}$: Body acceleration. In this case generated by the eKart motor (m/s^2)

$\sum F_t$: This is the force used to accelerate the vehicle, which is the unknown variable (N)

$\sum F_b$: Braking forces like wind resistance or road inclination, considered negligible in this case (N)

m: Vehicle mass (kg)

The "Motor block" computes what the relation between Torque and Force (Ft) is depending on vehicle´s speed. One of the main characteristics of a Permanent Magnet Synchronous Motor (PMSM) is the fact that it can deliver constant torque from 0 rpm up to what is called the Base Speed [6]. From that motor speed onwards, delivered torque decreases as it can be seen below:

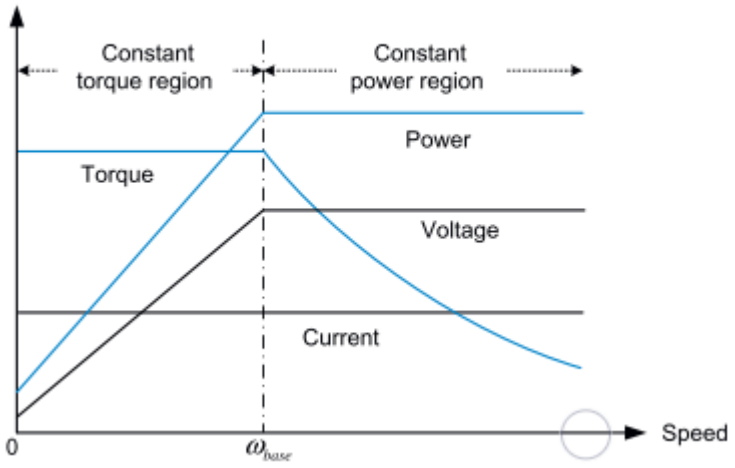

Figure 13: Typical PMSM performance curves [6]

In this case, the assumed Base Speed for the motor has been 49.62 kph [3]. This value has been calculated by considering current BRB AM2 eKart´s Motor characteristics, gear ratio and also tyre size.

Therefore, the Motor Block outputs a constant Force value below the Base Speed and lower Force values when vehicle speed increases.

That Force is used to accelerate the vehicle as per expression (1) and also allows the model the obtain the mechanical Power:

$$P = \frac{dW}{dt} = F_t \times v \tag{3}$$

Where:

W= Work generated by vehicle (J)
F= Force (N)
dt=Time (s)
v = Vehicle speed (m/s)

Once power is known, the current coming out of a battery pack can be figured out considering we know the nominal voltage of the pack is 48V:

$$P = V \times I \rightarrow I = \frac{P}{V} \tag{5}$$

In which:

P = Power (W)
V = Voltage (V)
I = Current (A)

Figure 13 also shows that power keeps increasing up to the base speed, from which it is constant. From a battery power delivery perspective, this means that current will be increasing up to the base speed, at which point it will be constant. This is because voltage can be considered constant (although it decreases as SOC lowers) and therefore, current must increase if power wants to get larger.

Also, it is worth noting that when calculating eMotor´s current, a generic efficiency of 0.9 has been assumed for both the eMotor and the inverter of the vehicle.

Therefore, following these steps allows us to obtain a theoretical current profile the pack supplies while driving the e-kart on the track. This profile can be seen below:

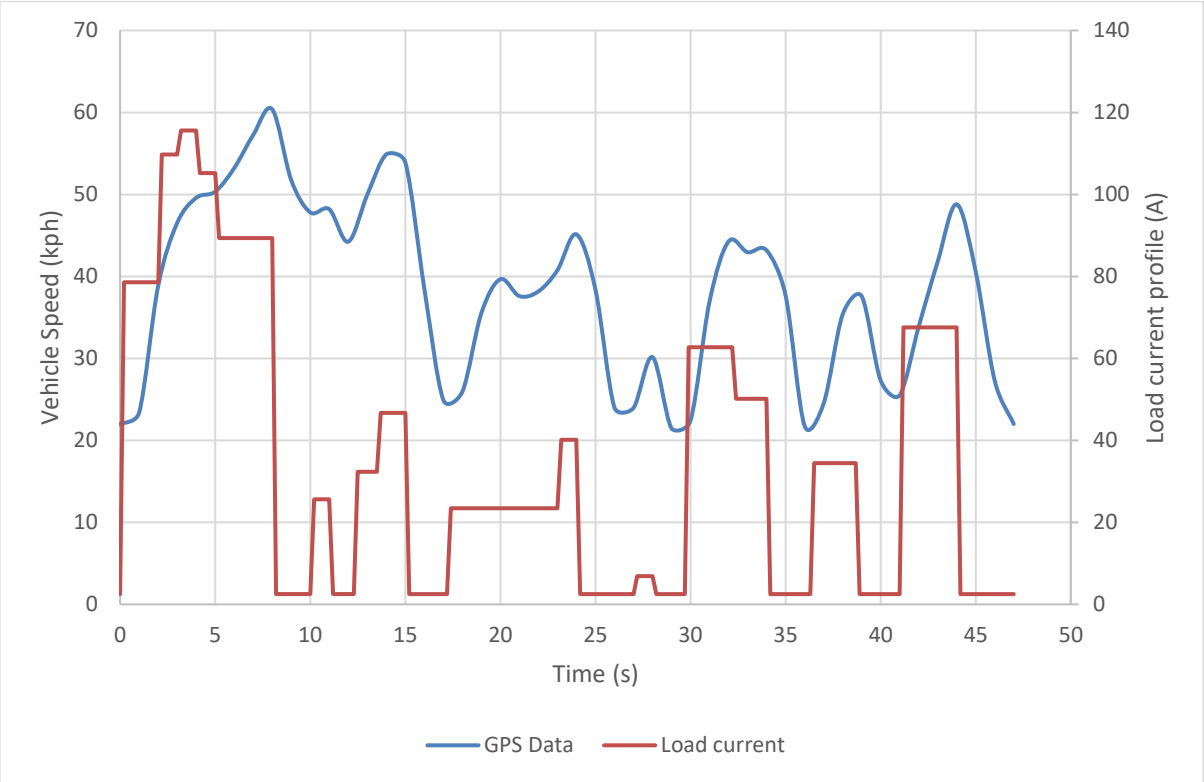

Figure 14: Load current and speed profile versus time.

This is the actual current profile which has been run repeatedly during the tests, both during the pre-conditioning cycle and during the test after cells were charged up. Both pre-conditioning and test consisted of a stint of 30 consecutive laps. Further consecutive laps were not considered as Cell Voltage would get close to the 2.5V lower limit.

This profile is a simplification of what would happen in reality. The fact that GPS data was logged at 1Hz and that the DC supply used to command the EL had a limited number of programmable nodes, means that current values applied are constant for longer periods than one second. This is to make sure DC supply programmable node limit is not reached.

3.3 LFP Battery Pack considerations:

For the execution of this work, several Li-Ion LFP cell sizes were considered. LFP cells come in a wide range of capacities and therefore it is possible to create a one string pack or alternatively use lower capacity cells and have several strings in parallel.

The real eKart features a 48V/90Ah Li-Ion pack so ideally, a pack of similar capacity should be considered for this work.

One option would be to purchase 90Ah LFP cells and create a series string in order to reach the nominal 48V for the pack. However, this would have required the purchase of at least two 90Ah cells for testing, which is a significant cost for this project.

Another option has been to borrow some 40Ah LFP cells from a current project within URV. This has allowed the Author to test LFP cells quicker and at no cost. Considering this, an hypothetical pack with two parallel strings of 40Ah cells is assumed as it gives a capacity which is close enough to the real eKart application.

Having said this, this fact implies that current values obtained from calculations have been divided by two in order to simulate two parallel strings.

4 Li-Ion LFP Cell Tests

This section details which tests have been completed during this project. As previously mentioned, one of the main aims of this work is to prove that LFP cells would be able to deliver the right performance for an e-Kart application. Other than that, two cells have been tested in different positions in order to understand whether cell positioning plays an important role when it comes to thermal performance. Considering the above, the four different configurations which have been tested are explained below.

4.1 Cell configurations

4.1.1 Side-by-side (1)

The first configuration was to place one cell next to each other, in contact as shown below. This was chosen as it is a configuration that offers very good energy density at pack level.

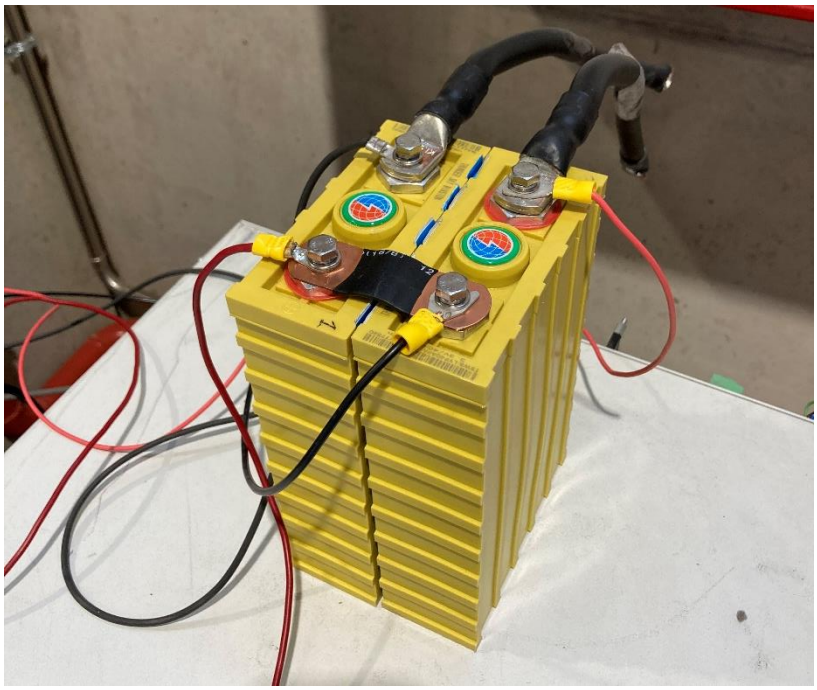

Figure 15: Two series-connected prismatic LFP cells

If looking carefully, one can spot that the two cells above are connector in Series. This was done in order to avoid having control issues with the electronic load. More details can be found in Appendix B.

4.1.2 Side-by-side non-contact (2)

Next option was to simply separate cells so there was no contact between them. The idea behind this was to check whether increasing the surface area available for cooling would make a substantial difference or not. In order to connect Cells with an increased distance, an aluminium bus bar was fabricated.

Figure 16: Setup of the Cells when tested on the second configuration

Please note that a Polycarbonate box was also fabricated and used during all tests in order to simulate the Battery Pack casing.

4.1.3 Side-by-side with Heat sinks (3)

This third step aimed at potentially improving the cooling by adding one heat sink plate to each cell. The type of heat sink used increases significantly the cooling surface and therefore, it can potentially help getting rid of excess heat.

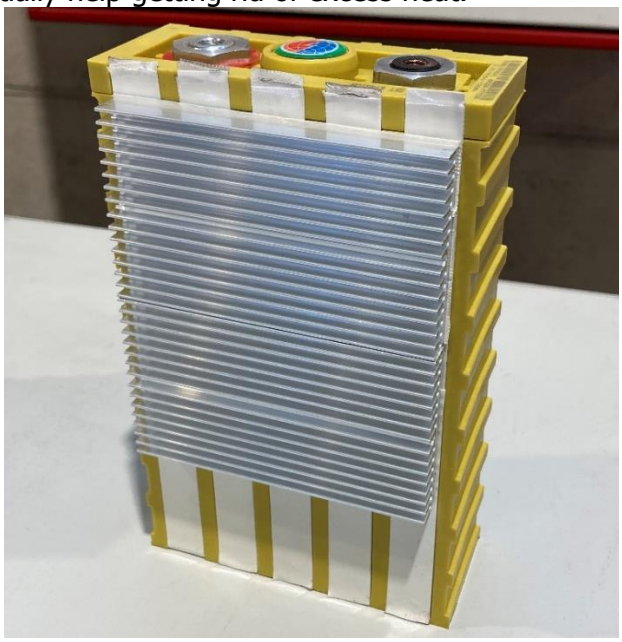

Figure 17: Detail of a heat sink plate attached to a Cell

4.1.4 Side-by-side, heat sinks and cooling fan (4)

The last iteration was to add an electric cooling fan in order to boost heat dissipation with forced air flowing around the cells. Cooling fans are widely used for cooling purposes as they maximise the effect of radiators (any car on our roads has got more than one cooling fan). The setup is shown below:

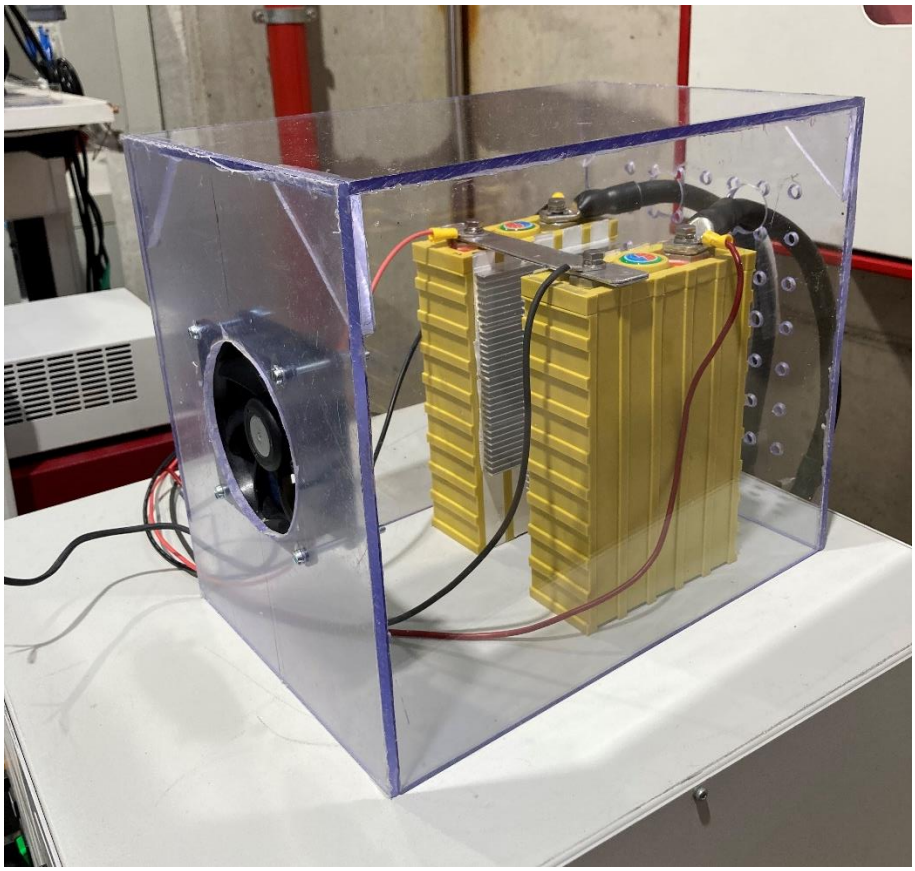

Figure 18: Full setup with cooling fan being used

4.2 Test steps

The same test was run on all configurations and cell temperatures were checked afterwards. In order to ensure a very similar starting point, cells were pre-conditioned in the same way for every test. The pre-conditioning and test steps are described below:

1. Both cells would be at max SOC at beginning of day. It is worth mentioning that cells were charged manually and at a slow rate (0.5C and then at lower rates until max voltage would be reached). Charging a cell manually requires a lot of attention in order to avoid over-charging and additionally, it is difficult to ensure that both cells get charged to the same SOC. On the other hand, following the same process during each charge phase ensures the reached SOC is reasonably similar.

2. Cells were connected to the EL and a discharge cycle consisting of 30 laps was run. This run was considered a pre-conditioning cycle.

3. Once completed, both cells would be charged fully. In this step, it is also worth noting that cells would be charged one after the other due to the equipment available.

4. After the previous step, cells would be discharged again running the same 30 lap cycle. It was decided to limit the number of laps to 30 because when performing more laps, voltage would drop very close to the lower limit.

5. Once completed, temperature would be checked by using a thermal camera. Some pictures were taken to check temperature distribution around cells and also the maximum temperature was recorded. These results can be found in the results´ section.

6. After that, cells would be charged again in preparation for the next test. Due to the high thermal inertia of Li-Ion cells [12], tests were done with a time gap of at least 24 hours. This was done to improve repeatability while testing.

4.3 Test setup

4.3.1 Setup components

The following section describes the laboratory equipment used to perform the different discharge tests. Firstly, a schematic of the setup is presented:

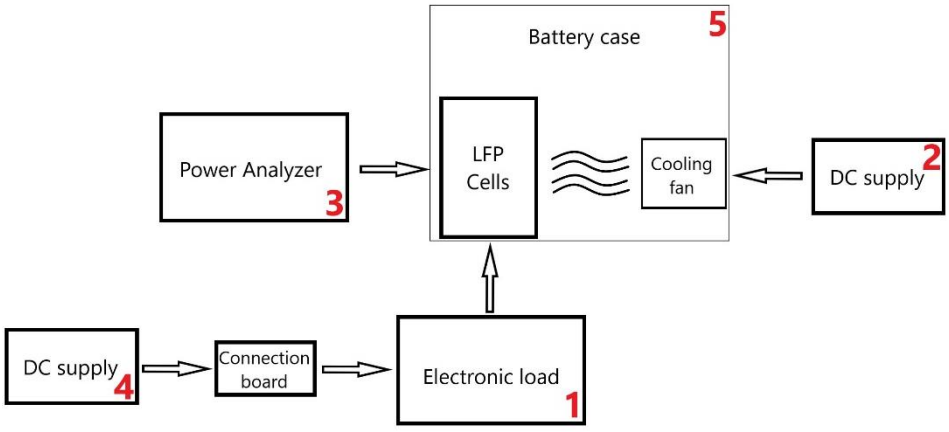

Figure 19: Schematic of the test setup

Also, an image is shown below so all elements can be identified:

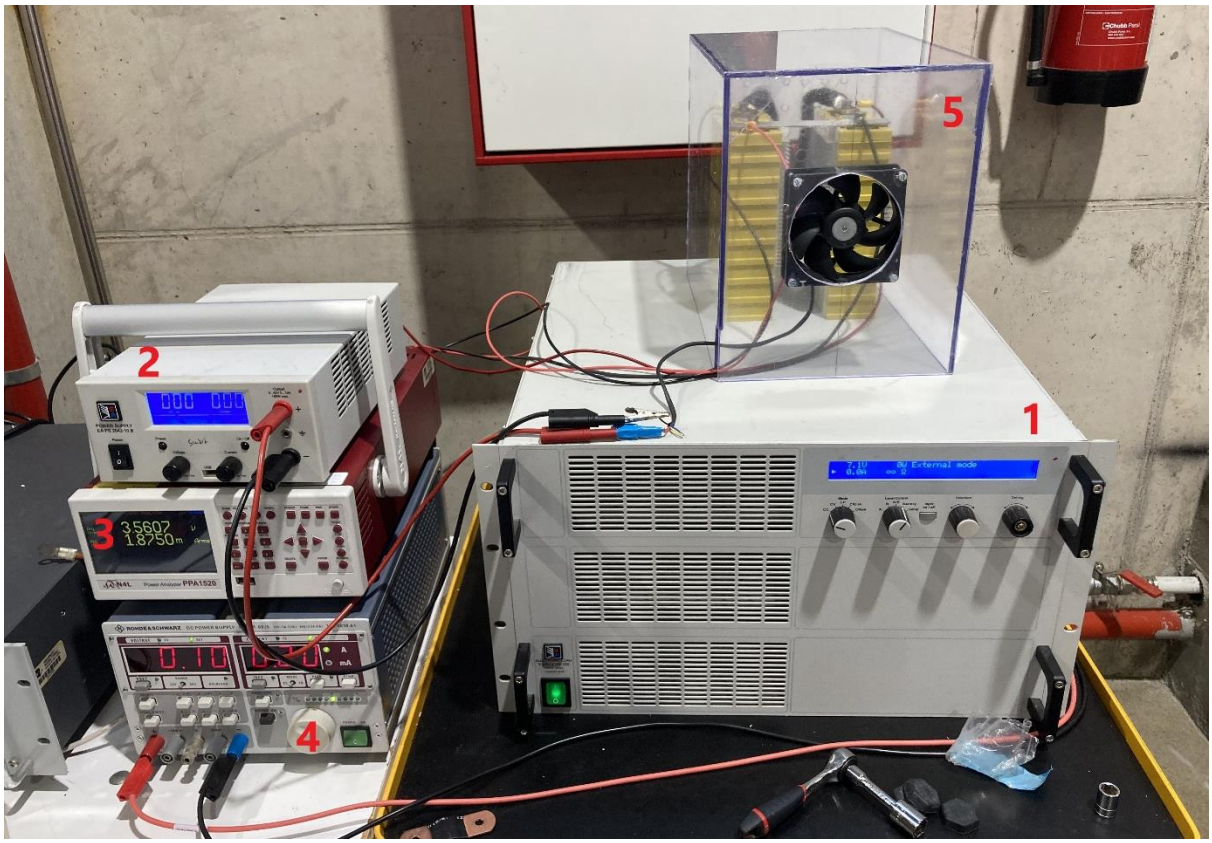

Figure 20: Equipment used in URV´s Power Electronics laboratory

4.3.1.1 Unidirectional Electronic Load:

This electronic load (EL) is the unit which discharges cells as specified. It can be controlled remotely using various methods like a DC supply. The EL used in this project has a current limit of 300A and is unidirectional, so it can only operate as a load. Bidirectional ELs also have the capability of operating as power supplies.

4.3.1.2 DC Supply:

Regular DC power supply used to power up the cooling fan.

4.3.1.3 Power Analyzer:

This is a power analyzer which has been used to log cell voltages during discharge tests. It can be controlled remotely via a laptop and it has the capability of exporting data directly to a spreadsheet.

4.3.1.4 Programmable DC supply:

This other DC supply has been used to control the EL remotely. A waveform can be programmed within its memory and then it can be set to run repetitively. This waveform is simply a set of voltage and time points which form a voltage profile depending on time. The voltage coming out of the supply is then interpreted by the EL and so the

desired current is drawn from cells. The waveform must be scaled between 0 and 10V, being 0V equivalent to a current draw of 0A and 10V being equivalent to 300A.

4.3.1.5 Box with cooling fan mounted

This box was made in order to simulate cells being inside a battery pack and also to make the fan operation more representative. Holes are present at the back so air can travel around the cells and exit the casing.

4.3.2 Connection board

Additionally, an electric circuit was built using a test board in order to make the interface between the DC supply and the EL:

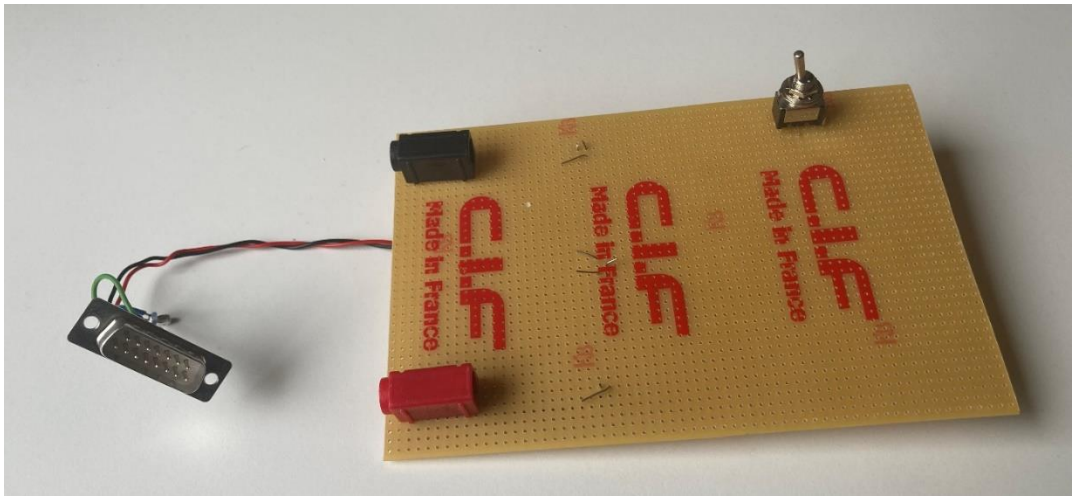

Figure 21: Electronic load bespoke remote control connection board

This board featured the following main components:

- 15 pin D-sub connector in order to connect to the EL.
- Positive and negative “banana” type connectors to connect the DC supply to the board.
- Manual switch so the EL´s remote control functionality can be manually switched ON and OFF.

Behind the board and for safety reasons, a voltage divider circuit was made in order to make sure no current would flow from the DC supply to the EL. This was made to ensure the EL could not be damaged. An electrical schematic of the circuit is shown below:

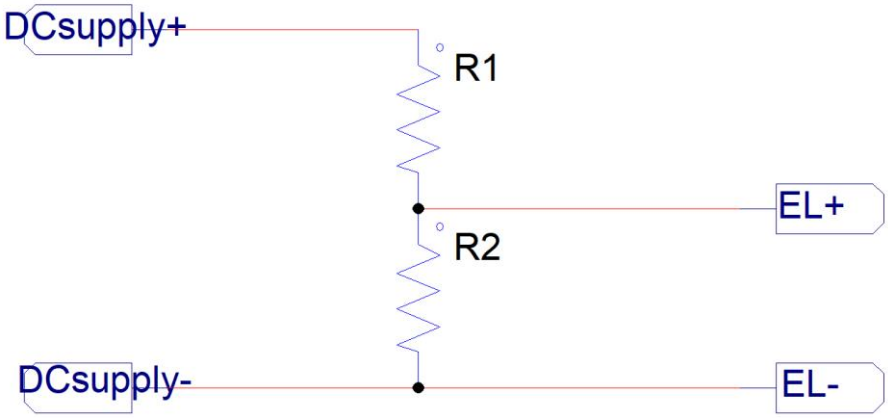

Figure 22: Voltage divider schematic

Both resistors are the same (1 kOhm in this case), which means the voltage drop the Electronic Load sees is half the voltage from the DC supply. This must be considered when programming the DC supply otherwise, current figures would be half the expected.

Using 1 kOhm resistors ensures the current flowing in this circuit will be very small and therefore, chances of damaging the EL are minimal.

Additionally, the table below describes what each pin on the D-sub connector is used for:

Pin	Name	Type[2]	Description	Level	Electrical specifications
1	VSEL	AI	Set value for voltage	0…10V, corresponds to 0..100% of U_{Nom}	Accuracy typically 0.1% Input impedance Ri > 40k…100K
2	CSEL	AI	Set value for current	0…10V, corresponds to 0..100% of I_{Nom}	
3	PSEL	AI	Set value for power	0…10V, corresponds to 0..100% of P_{Nom}	
4	RSEL	AI	Set value for resistance	0…10V, corresponds to 0..100% of R_{Nom}	
5	AGND	POT	Reference potential for analogue signals		For VSEL, CSEL, PSEL, RSEL, VMON, CMON, PMON and VREF
6	DGND	POT	Reference potential for digital signals		For control and error signals
7	Remote	DI	Selection internel / external	External = LOW (U_{Low} <1V) Internal = HIGH (U_{High} > 4V) or open	U range = 0 …30V I_{Max} = -1mA at 5V $U_{Low\ to\ High\ typ.}$ = 3V Sender: open collector against DGND
8	Rem-SB	DI	Load input on/off	OFF = LOW (U_{Low} <1V) ON = HIGH (U_{High} > 4V) or open	
9	VMON	AO	Actual value of voltage	0…10V correspond to 0..100% of U_{Nom}	Accuracy typically 0.1% at I_{Max} = +2mA Short-circuit-proof against AGND
10	CMON	AO	Istwert Strom	0…10V correspond to 0..100% of I_{Nom}	
11	VREF	AO	Reference voltage	10V	Accuracy typically 0.1% at I_{Max} = +5mA Short-circuit-proof against AGND
12	R-active	DI	Selection R=on / R=off [1]	R regulation = off = LOW (U_{Low} <1V) R regulation = on = HIGH (U_{High} > 4V) or open	U range = 0 …30V I_{Max} = -1mA at 5V $U_{Low\ to\ High\ typ.}$ = 3V Sender: open collector against DGND
13	R-Range	DI	Select resistance range [4]	R_{Max} = resistance range 2 = LOW (U_{Low} <1V) R_{Max} = resistance range 1 = HIGH (U_{High} > 4V) or open	
14	Trigger In	DI	Trigger input [3]	triggers A->B = LOW (U_{Low} < 1V) triggers B->A = HIGH (U_{High} >4V) or open	
15	OT / OVP	DO	Overtemperature/Overvoltage	OT or OVP = HIGH (U_{High} > 4V) no OT or OVP = LOW (U_{Low} < 1V)	Quasi open collector with pull-up against +15V At 15V at this output there will be max. +1.5mA Short-circuit-proof against DGND Receiver: U_{Low} <1V, U_{High} > 4V

Figure 23: Electronic load 15-pin DSUB connector pinout

The pins highlighted correspond to the pins which have been used in this configuration. The following connections have been made:

- Pin 2: Connected to "EL+" from figure 21. Positive wire coming from DC supply controller.
- Pin 5: Connected to "EL-" from figure 21. Negative wire coming from DC supply controller.
- Pins 3 and 11: In order to avoid having power limitations.
- Pins 5 and 12: So Resistance regulation functionality is not used.
- Pins 5 and 7: These two pins were also joined but, in this case, a manual switch was added in series so the "Remote Control" mode could be switched ON/OFF as desired.

5 Results and analysis

5.1 Thermal performance

In this section, all results from the tests performed are presented. These tests were completed on separate dates to allow cells to completely cool down. Also, it is worth mentioning that ambient temperature inside the laboratory was always regulated to the same target temperature. Furthermore, the pre-conditioning process was completed exactly in the same way for each test. This fact also contributed to having a similar starting temperature at each test.

The table below summarises results from a thermal point of view:

Test configuration	Description	Start temperature (°C)	End temperature (°C)	Temperature Delta (°C)	Delta temperature to Tmax Cell (°C)
1	Cells side-by-side	30.2	35.6	5.4	44.4
2	1 + Air gap between Cells	31.2	34	2.8	46
3	2 + heat sinks	30	34	4	46
4	3 + cooling fan	31.3	31.6	0.3	48.4

From the above table, the following can be stated:

- From a thermal point of view, the worst configuration is the first one, which is having cells in contact with each other. This was the test with the highest delta temperature between start and end of test.
- Allowing for a small gap in-between cells already offers a significant gain in thermal performance.

- After any of the tests, the highest cell temperature was still far away from the 80°C maximum continuous operational temperature of this LFP cell (according to the Technical Specification attached in Appendix A).
- Heat sinks do not seem to improve heat transfer, at least when a cooling fan is not present.
- The highest temperature within a cell tends to be its very centre. On Figure 29 it can be clearly seen that hottest point within the cell is its nucleus.
- Finally, a cooling fan proves to be very useful when it comes to cell cooling. Delta temperature during configuration 4 was only 0.3°C.

Also, pictures showing temperature distribution at the end of each test are shown below:

5.1.1 Configuration 1

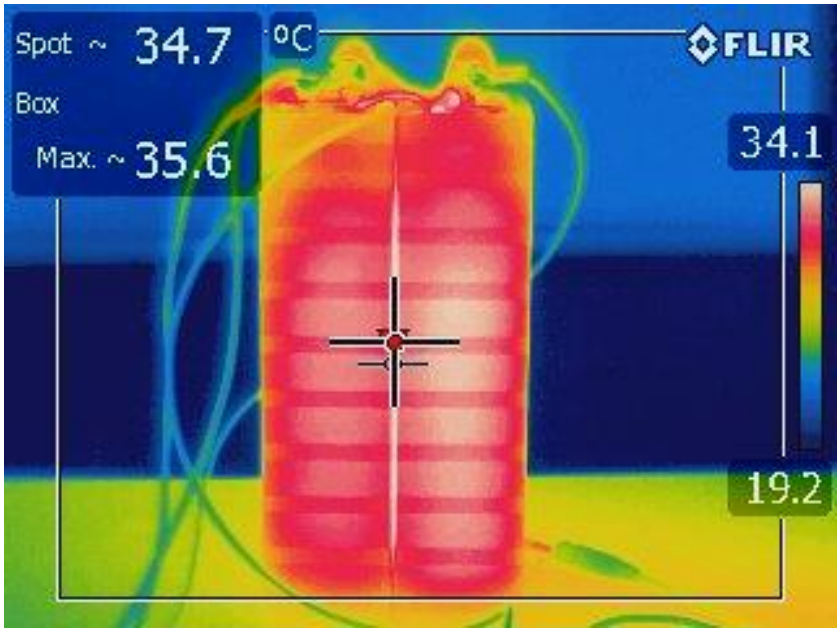

Figure 24: Thermal results configuration 1 – side view

Clearly, the fact that cells are in contact side-by-side creates an area where heat rejection minimal. This is potentially the reason why the highest temperature was found on this area. On the other hand, it is worth noting that the highest temperature within one of the cells was very close to the temperature shown above. More specifically, the difference was only of 0.6 °C (see image below).

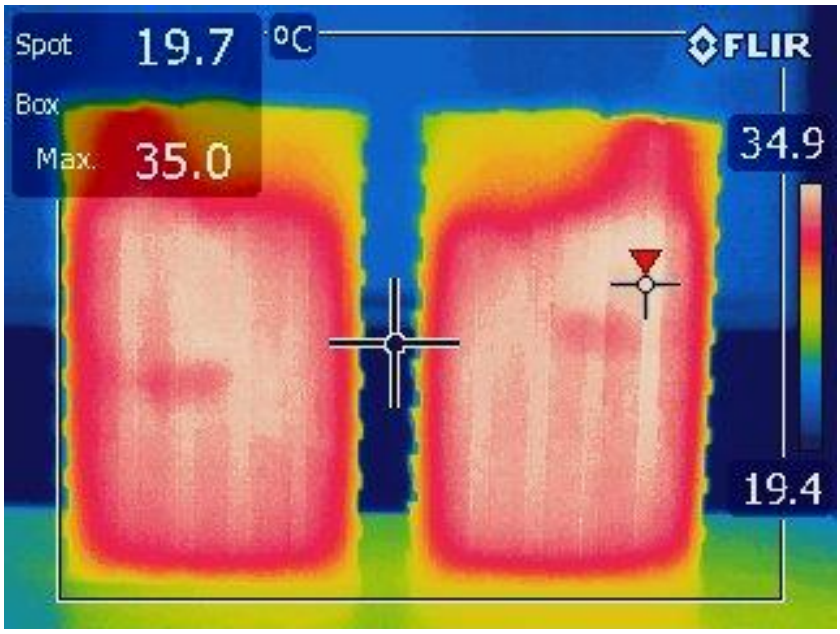

Figure 25: Thermal results configuration 1 – front view

5.1.2 Configuration 2

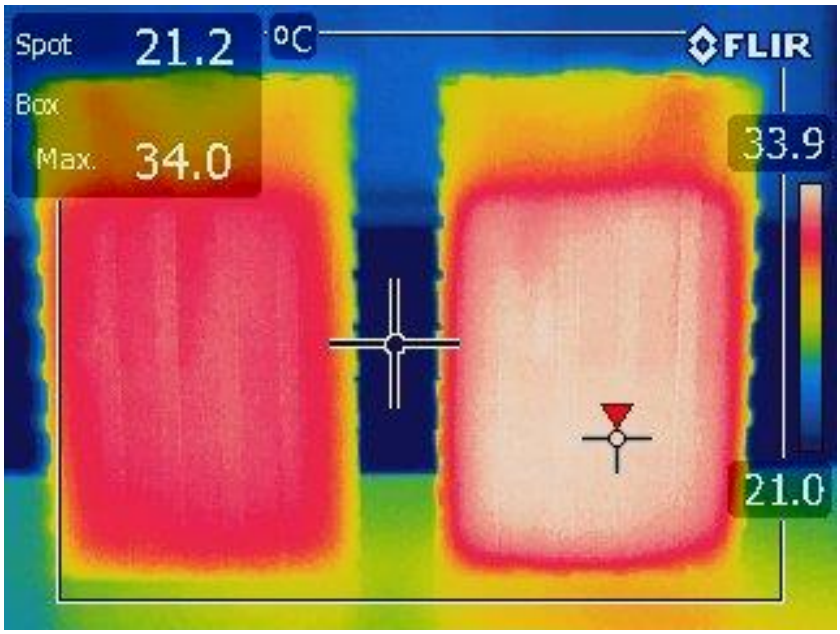

Figure 26: Thermal results configuration 2 – front view

As mentioned, maximum temperature after the test was slightly reduced by separating cells. Additionally, it is also possible to see a small difference in temperature between both cells. This is most probably because cell on the right was charged after the other cell. The fact that this was not seen after Test 1 could be because heat was being transferred between cells until they equalized.

5.1.3 Configuration 3

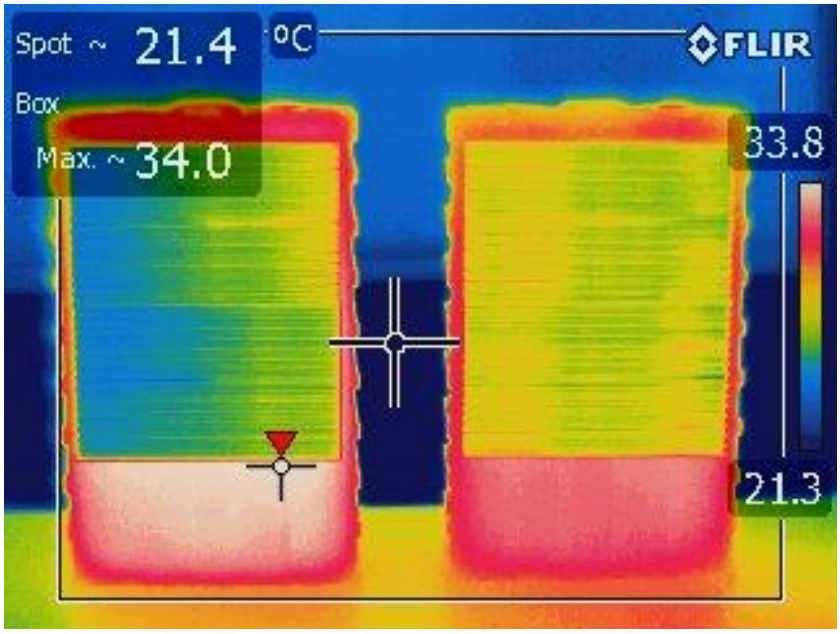

Figure 27: Thermal results configuration 3 – front view

Adding heat sinks to one of the sides of both cells did not have a significant effect on heat rejection. In fact, maximum temperature after the test was the same as with Configuration 2 (on which heat sinks were not installed). When looking at the picture above, it can be seen how there is a significant temperature gradient on the heat sink surface. The fact the cell on the left exhibits low (blue) temperature areas on about half of the heat sink surface potentially means that area of the heat sink did not stick correctly to the cell surface. When installing the heat sinks it was observed that the sides of cells were not completely flat and therefore, fixing heat sinks with an adhesive tape may not have resulted in a homogeneous adhesion.

5.1.4 Configuration 4

As shown in picture 20, that test was run whilst using a cooling fan. Results indicate that this method of cooling down cells is very effective.

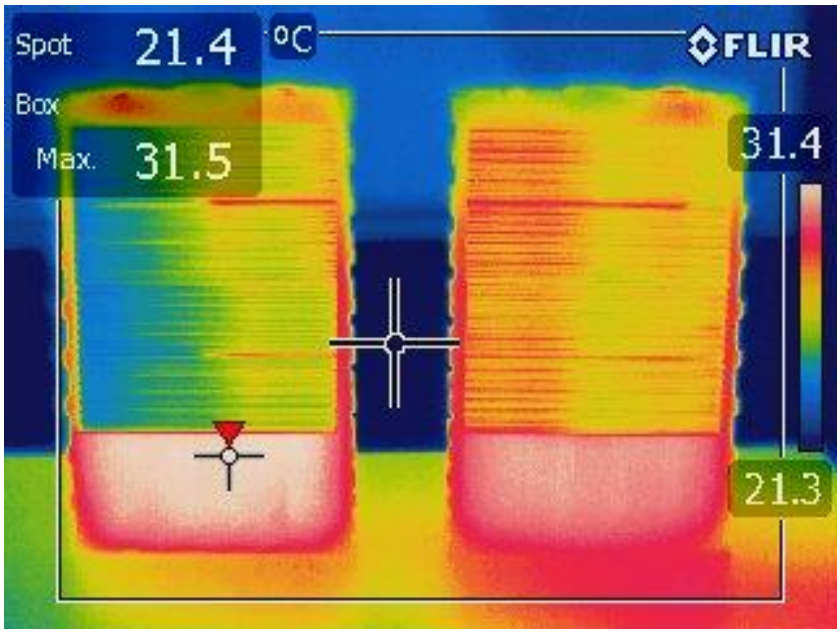

Figure 28: Thermal results configuration 4 – front view

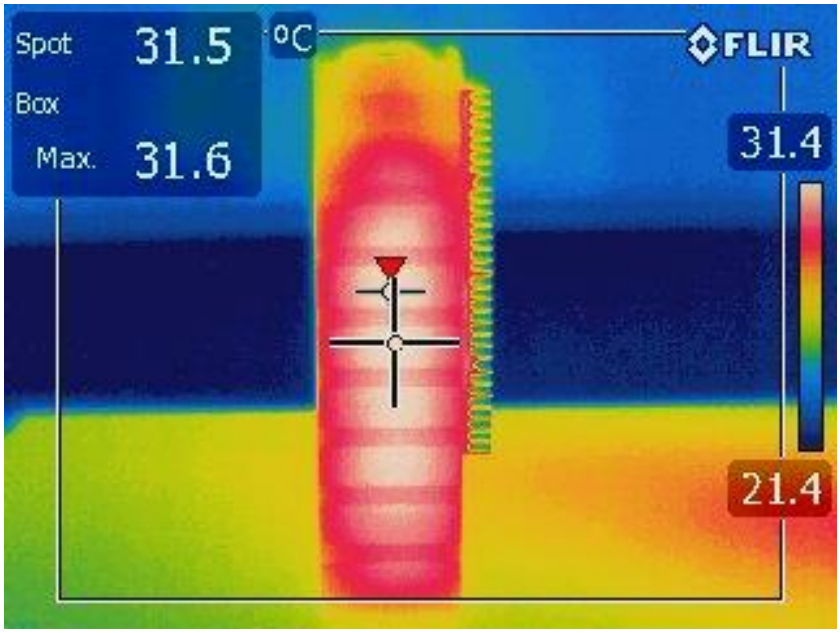

Figure 29: Thermal results configuration 4 – side view

31.6°C was the highest cell temperature found after this last test. This is only 0.3°C higher than the maximum temperature recorded at the beginning of that test.

Additionally, it is worth noting how the highest temperature on the cell is right in the middle of it and a negative temperature gradient is seen when getting closer to the sides of the cell. Potentially, this effect is increased when using a cooling fan as forced air is impacting directly to the external's cell surface.

5.2 Electrical performance

This section presents the results obtained after having logged cell voltages with the power analyser unit. The next four charts show cell voltage behaviour of both cells for all tested configurations.

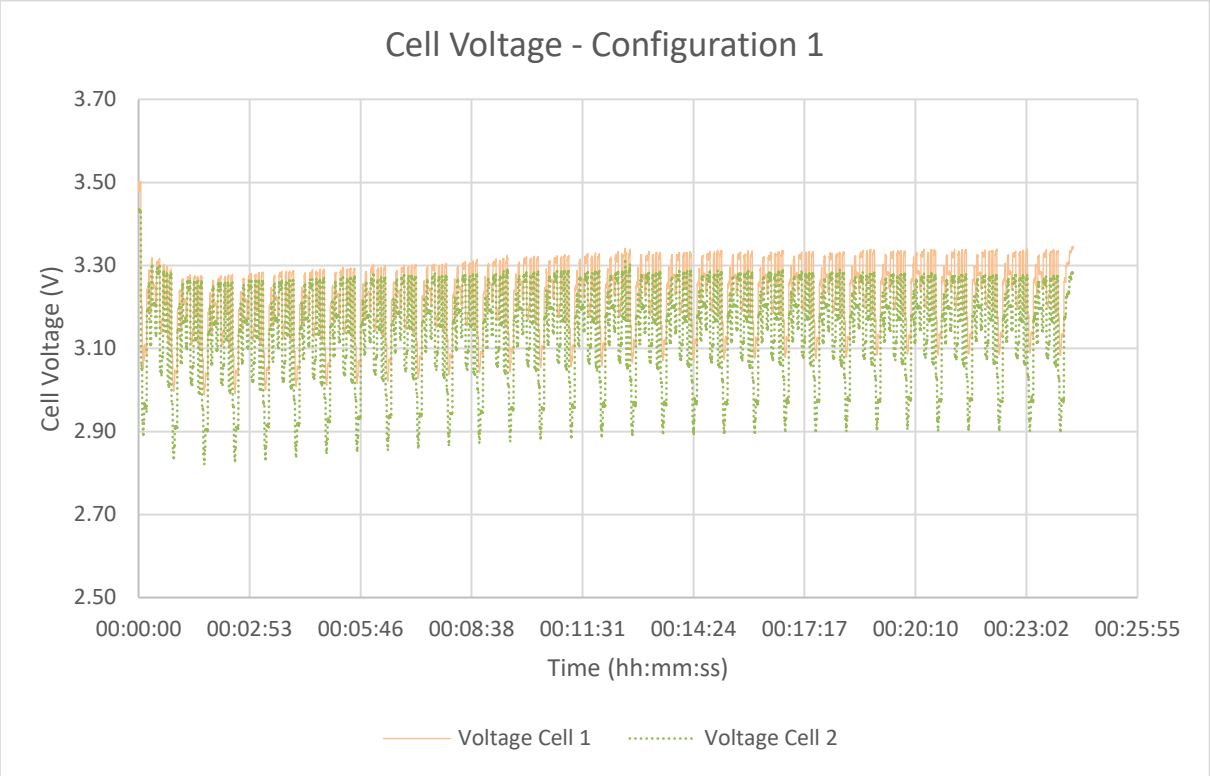

In the case of configuration 1, Cell 2 exhibited significant voltage drops during the test. It can be seen that during the biggest drop, voltage reaches 2.9V when in the case of cell 1, the voltage drops to about 3.1V. A possible reason for this behaviour could be the fact that Cell 2´s SOC at the start of the test was considerably lower. In fact, at the very beginning of the test, Cell 1 is at 3.5V (fully charged) whereas Cell 2 is at around 3.42V. This seems a small difference but it could explain part of the described behaviour.

Additionally, Cell 2 stabilised rapidly, possibly because it had been charged prior to Cell 1. Charging cells one after the other also means there will be some temperature differences. Cell internal resistance also changes depending on the temperature so this fact can also contribute to the described behaviour.

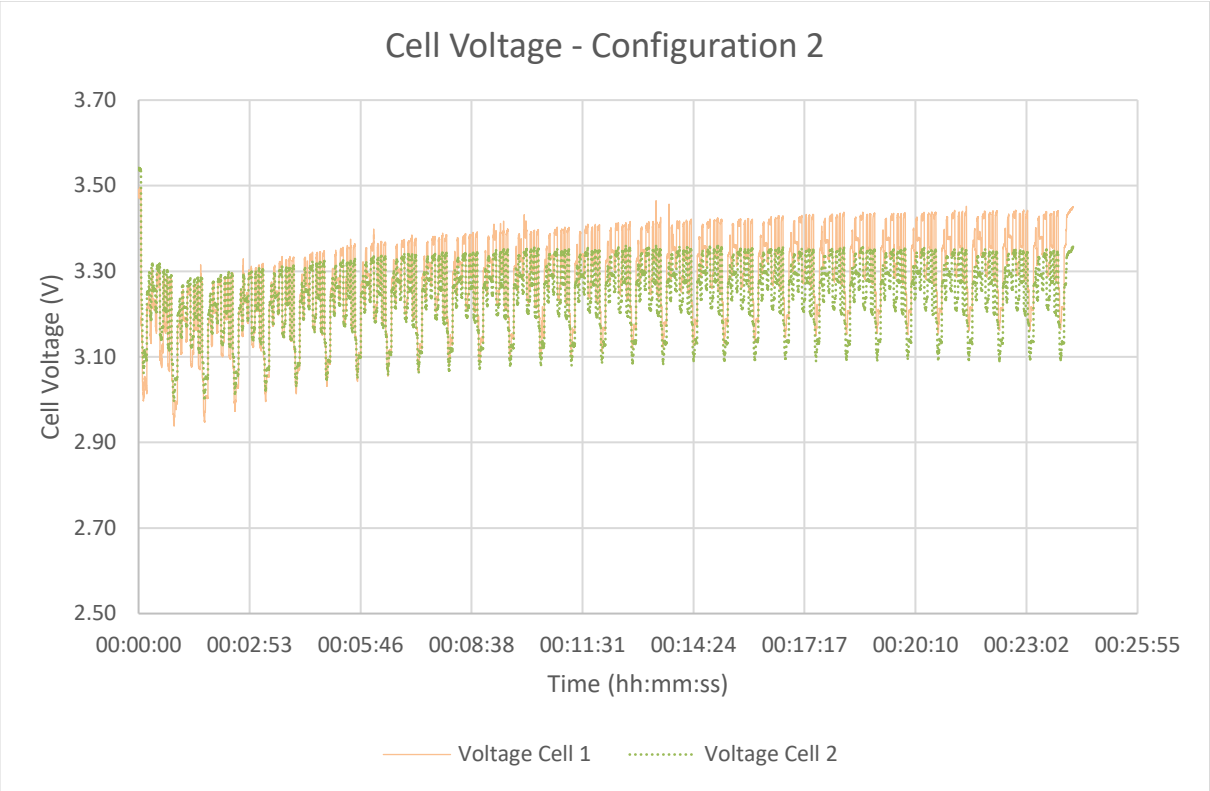

During the second test, Cell 2 was again working at lower voltages compared to Cell 1. Despite the initial voltage was higher, it then stabilised to lower voltage figures. Also, for an unknown reason, during this test it took longer for both cells to stabilise (specially Cell 1).

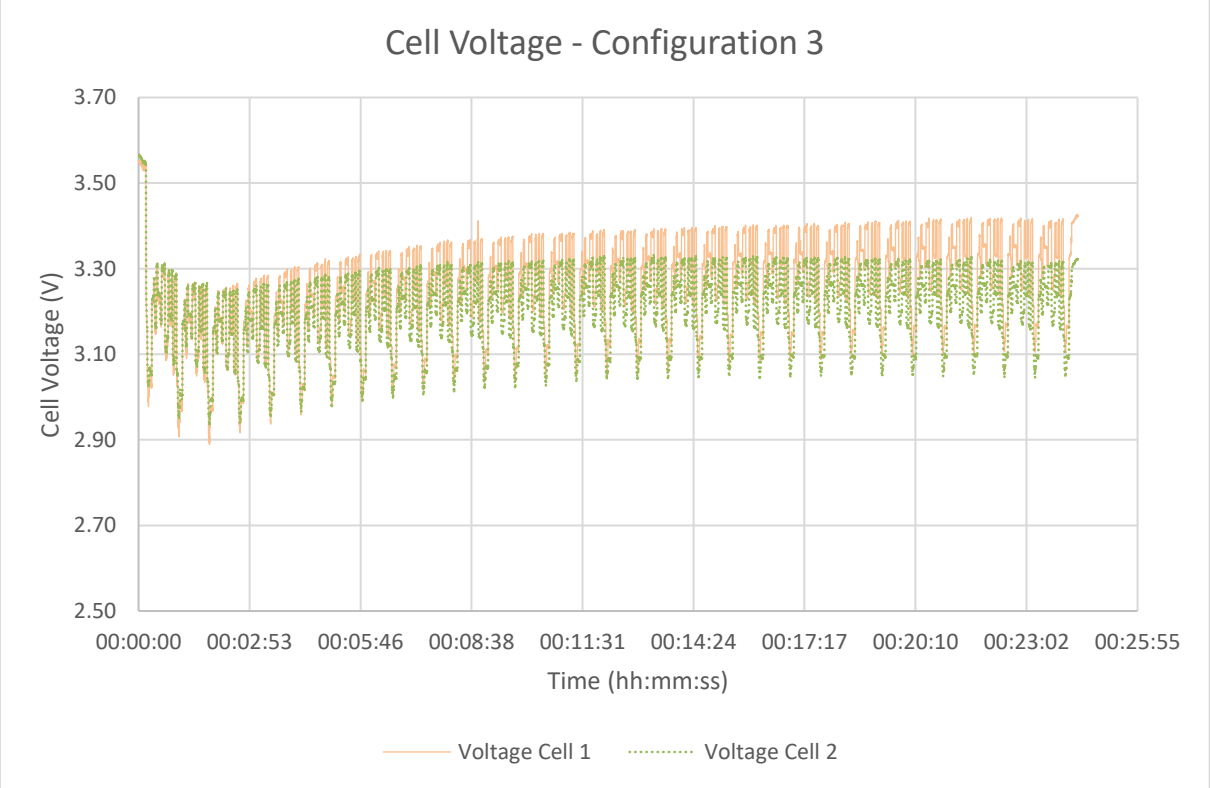

Configuration 3 showed very similar results to the prior configuration. Therefore, no additional electrical behaviour differences were observed.

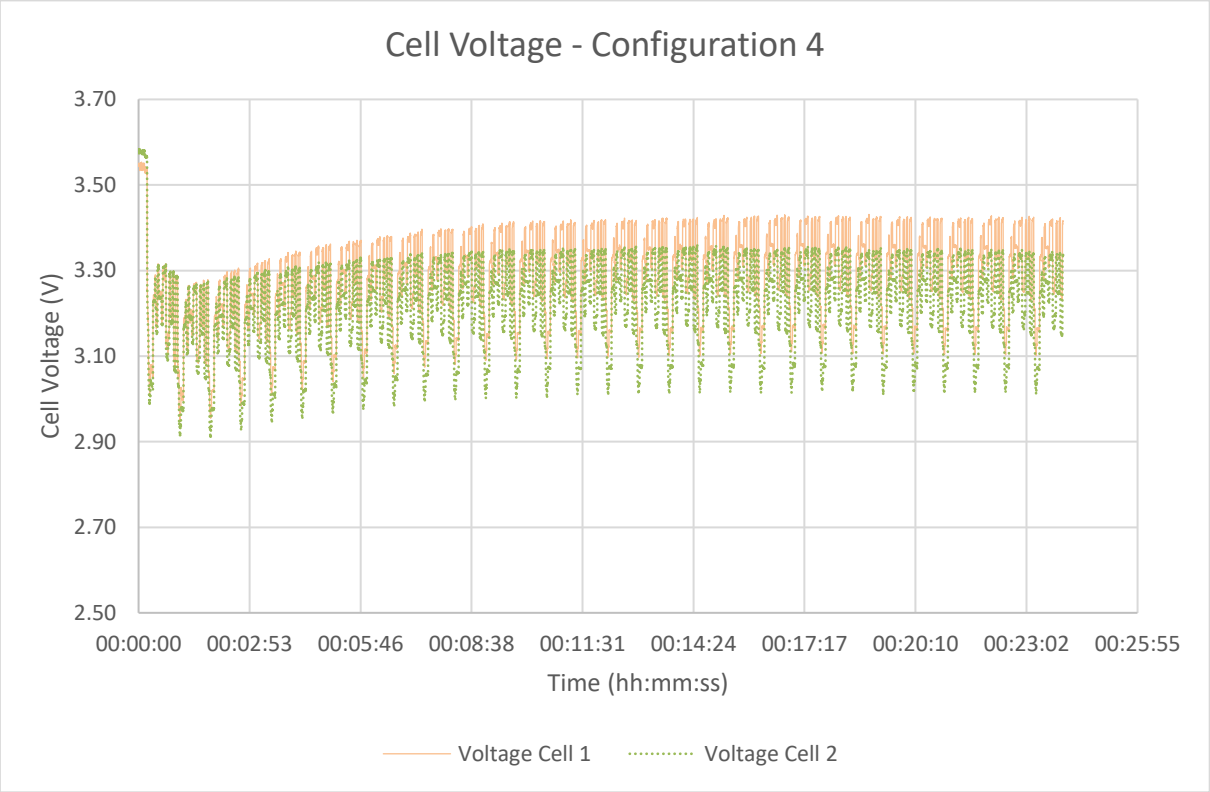

The last configuration continued to confirm that Cell 2 was operating at lower voltages. Again, even if the starting voltage was higher.

One other behaviour worth mentioning is that voltage difference between cells during the test kept increasing. During any of the tests, cell voltage is very similar during the first minute and then the difference between operating voltages increased during the test. A chart from one of the tests is shown below:

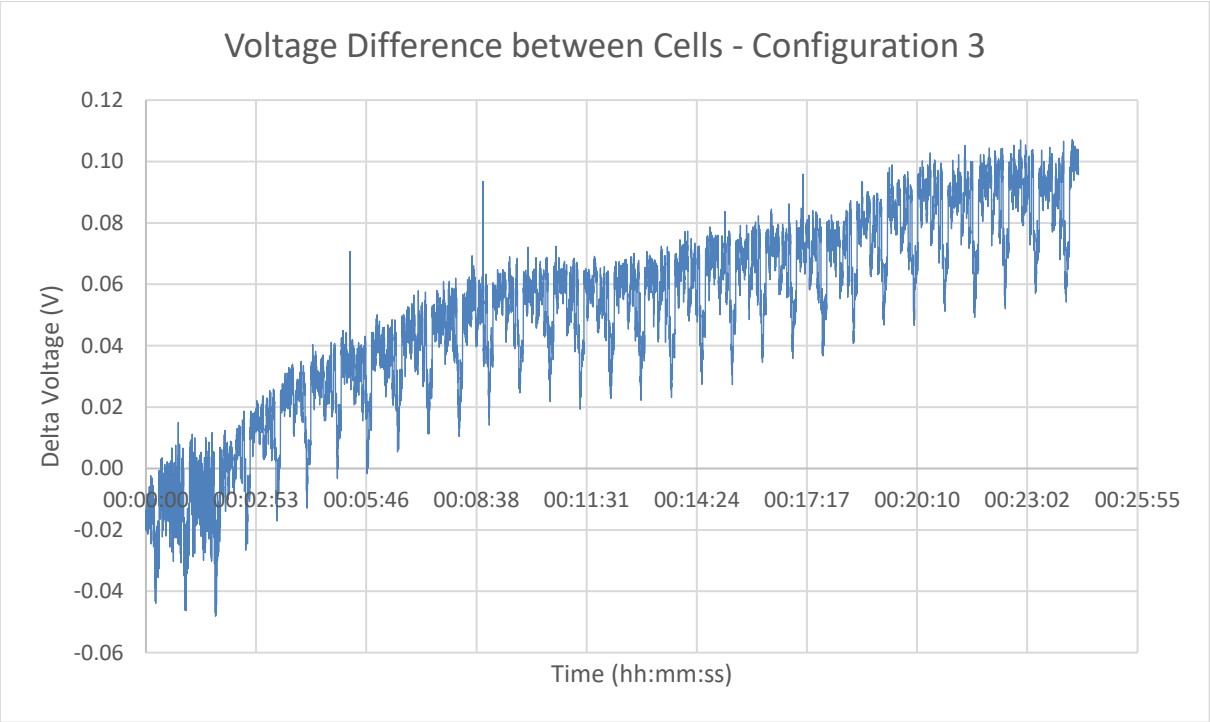

Interestingly, test with Configuration 4 showed stabilisation halfway during the test:

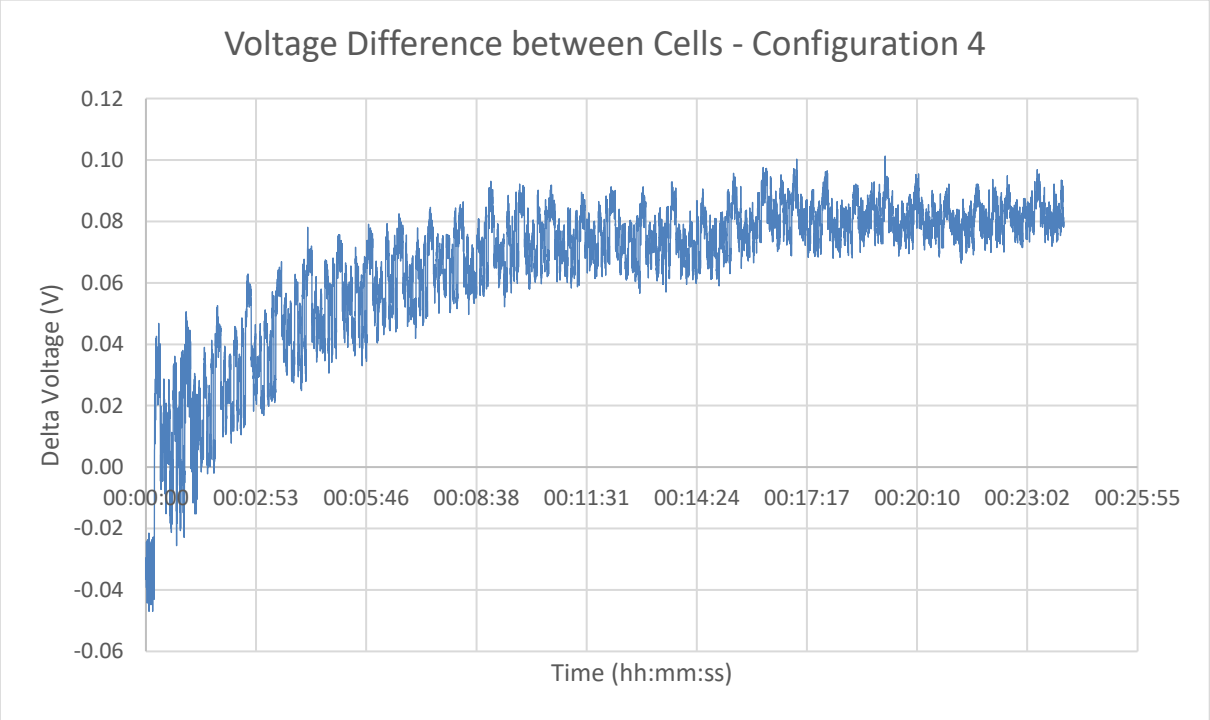

The reason for this behaviour could be a combination of having different cell conditions, mainly SOC and temperature.

6 Battery Pack configuration proposal

After having analysed the results of tests performed, this section proposes a configuration for a potential pack which could be built and used on an eKart.

6.1 Cell selection

As mentioned previously, the tests performed during this Project were completed using 40 Ah cells (because of availability reasons). Testing proved that virtually, around 30 laps on a karting circuit could be completed on a single charge when using these cells. A karting session for recreational use is usually around 10 minutes long, during which 10-15 Laps can potentially be completed. This is obviously highly related to the track length and other factors too.

On the other hand, the current BRB eKart has a battery pack of 90 Ah, which is more than twice the size of the used cells.

Considering the above two points, a potential cell candidate could have a capacity between 50 and 90 Ah. This would ensure enough capacity to last a recreational karting session and also have decent capacity to ensure a longer cell life (less DOD at each session).

The same manufacturer of the tested cells also offers versions of 60Ah and 90Ah, weighing 2.3kg and 3kg respectively. Using 90Ah cells would imply having a battery pack of 45kg plus all the casing, wires and battery management system components. This is deemed too heavy if compared to the current pack being used. On the other hand, 60Ah cells are a good option as they have a lower weight and additionally, they could deliver the required performance. Table below shows main characteristics of the Winston 60Ah LFP cell:

	60Ah Winston LFP Cell
Weight (kg)	2.3
Cycle life (n° of cycles)	+5000 (80% DOD)
Max discharge current (A)	600 (5 sec./minute)
Max charging current (A)	180
Max operating temperature (deg.C)	80

6.2 Pack configuration

The image below represents how fifteen 60Ah LFP cells could be placed inside a case with the same size as the current BRB AM2 pack's case. Image below represents how fifteen 60Ah LFP cells would fit inside the current dimensions of AM2's pack:

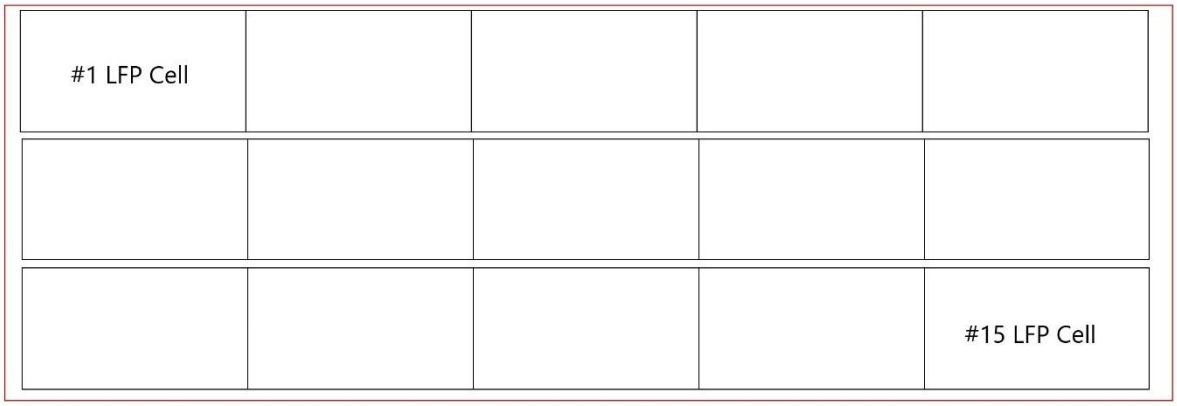

Figure 30: 60Ah LFP Cell arrangement inside BRB AM2 Pack.

There would even be the possibility to leave a small gap between cells to create a cooling channel. Effectively, a cooling fan could be installed on one side of the pack force air to circulate along the pack when necessary.

Regarding height, using the 60Ah cells would leave around 87mm gap to install cabling and BMS related components above the cells and below casing's upper cover.

On the other hand, this preliminary draft reveals that the fitment of 60Ah cells in the current casing would be significantly tight and therefore, it is probable that a small increase in casing size would be necessary.

6.3 Performance comparison against current BRB AM2 Pack

Table below compares the current pack installed on a BRB AM2 eKart against a theoretical pack built using 60 Ah LFP cells:

	BRB AM2 Pack (ternary Cells)	60Ah LFP Cell Pack
Battery capacity (kWh)	4.3	2.9
Cycle life	+10000 depending on DOD	+5000@ 80% DOD
Max current (A)	230	600 (6 sec./minute)
Weight (kg)	~25	~40
Safety	High	Highest
Max. Charging current (A)	100	180

From the table above, the following conclusions can be withdrawn:

- A 60Ah LFP pack would be able to deliver the performance of the current pack.
- Potentially more discharge/charge power would be available.
- A LFP pack would be heavier than the current solution.
- Using LFP chemistry would bring higher safety compared to current ternary chemistry.
- Range would be smaller than with the current solution.
- Regarding cycle life, it is difficult to tell but LFP is known for its higher life cycle compared to ternary chemistries like NMC or NCA.

LFP pack advantages like a higher safety or increased performance are quite strong reasons to seriously consider using LFP cells. Also, another of its strenghts is the much smaller number of cells to assemble and the fact that no welding is needed to connect cells.

One of the main drawbacks of using LFP cells though is the fact that pack's weight would be significantly higher because of its lower energy density. On the other hand, the fact that the eKart would be for a recreational application reduces the importance of achieving ultimate performance.

7 Conclusions

The work described above has led the author to obtain various conclusions based on the testing performed.

First of all and most importantly, the tested LFP cells can be considered to be adequate for the use in an eKart project. They can be discharged running virtual laps around a karting circuit without exhibiting thermal related issues and offering good performance. Even assuming some deviation between the calculations and reality, the author believes these cells can perfectly deliver enough energy to power an eKart and complete several consecutive laps.

Additionally, considering temperature at the end of each test was far away from maximum operating temperature, these cells could potentially deliver more power and still not reach their limit.

On the other hand, it is important to realise that due to having equipment availability limitations, discharge tests could not be tested together with fast charging operations. Fast charging is common on eKarting circuit because when there are lots of customers waiting to drive the vehicles there is no time for slow charging. Therefore, fast charging is regular and could potentially stress cells more than the actual driving. This is because fast charging means putting the cell under a constant high load. Cells were charged between tests at around 1C and in those conditions an increase in temperature was already notable. To put it into perspective, an eKart application would require charging at around 2C.

Another limitation when it comes to LFP cells is their lower energy density compared to other chemistries. A pack with 3.5-4 kWh would weight more than 40kg and that is something to consider in an eKart application. In any case, as mentioned in the Introduction, this may not be a limiting factor considering the proposed application is a recreational vehicle.

From the different configurations which were tested, the most important conclusion is the fact that a cooling fan has a significant positive effect when it comes to cooling performance. If a cooling fan is not an option, it is also advisable to slightly separate cells so they are not in contact at one of their sides. Doing so increases the surface area on which heat can be transferred.

8 Further steps

If the author was to continue working on this topic, these are the main activities which would be completed:

The first one would be to repeat tests but this time, a bidirectional Electronic Load would be used in order to simulate fast charging prior to running the virtual laps. If cells passed that test, that would give more confidence on the viability of these cells for this application.

Also, the charging process would be done with both cells connected in series, thus ensuring the same charge current would enter both cells.

Finally, a test with the cooling fan but no heat sinks would also be performed as it would allow to confirm whether it is worth using them or not. Related to this, surface adhesion of heat sinks would also be improved to ensure better cell to heat sink heat transfer.

9 References

[1] Bureau of Transportation Statistics (2022, June 21). “Hybrid-Electric, Plug-In Hybrid-Electric and Electric Vehicle Sales”
Available: https://www.bts.gov/content/gasoline-hybrid-and-electric-vehicle-sales

[2] Epec Engineered Technologies. “Battery Cell Comparison”
Available: https://www.epectec.com/batteries/cell-comparison.html

[3] Evea Kartmasters (2020, May 7). “EVEA - Motenergy ME1507 & Zapi BLE-4 PW 96V 700A on test bench.”
Available: https://www.youtube.com/watch?v=ux-R-OH9_Fo&t=1s

[4] Himax Electronics. “LiFePO4 Rechargeable Prismatic Battery”
Available: https://himaxelectronics.com/product-item/lifepo4-battery-cell-3-2v-200ah/

[5] International Energy Agency (2023). “Global EV Outlook 2023”. Available: https://iea.blob.core.windows.net/assets/dacf14d2-eabc-498a-8263-9f97fd5dc327/GEVO2023.pdf

[6] Kim, S., n.d. (2017) “Electric Motor Control: DC, AC and BLDC Motors.”

[7] Lombardo,T (2022, September 30). “Why EV manufacturers Are Switching from NMC to LFP”. Engineering.com.
Available: https://www.engineering.com/story/why-ev-manufacturers-are-switching-from-nmc-to-lfp-batteries

[8] Melançon, S. (2022, April 25). “Prismatic vs. Cylindrical Cells: What is the difference?” Laserax.
https://www.laserax.com/blog/prismatic-vs-cylindrical-cells

[9] N.Muralidharan, E.Self, M.Dixit, Z,Du et all (2022, January 22). “Next-Generation Cobalt-Free Cathodes – A prospective solution to the battery Industry´s Cobalt problem”. Wiley Online Library
Available: https://onlinelibrary.wiley.com/doi/10.1002/aenm.202103050

[10] Transport and environment (2020, April 21). “Does an electric vehicle emit less than a petrol or diesel?”.
Available: https://www.transportenvironment.org/discover/does-electric-vehicle-emit-less-petrol-or-diesel/

[11] S. Loveday (2021, December 2). “EV Battery Cell & Pack prices Dropping at surprising rate”. Available: https://insideevs.com/news/552010/electric-car-battery-prices-dropping/

[12] S.Wang, K.Li, Y.Tian, J.Wang et all (2019, May 25). “An experimental and numerical examination on the thermal inertia of a cylindrical lithium-ion power battery”. Applied Thermal Engineering. Vol.154, pp.676-685. Available: https://www.sciencedirect.com/science/article/abs/pii/S1359431118377494

[13] Volvo Cars (2021, November 1). “Carbon footprint report – Volvo C40 Recharge”.
Available: https://www.volvocars.com/images/v/-/media/Market-Assets/INTL/Applications/DotCom/PDF/C40/Volvo-C40-Recharge-LCA-report.pdf

[14] Worldsaid (2023, Jan 03). “Cobalt mines – Child labour in the Democratic Republic of the Congo”.
Available: https://www.worldsaid.com/node/1703

10 Apendix A – Li-Ion 40Ah LFP Technical Specifications

Specifications		
Model name	LFP040AHA	Alternative product marking TS-LFP40AHA, WB-LYP40AHA
Nominal voltage	3.3 V	Operating voltage under load is 3.0 V
Capacity	40 AH	+/- 5%
Operating voltage	max 4.0V - min 2.8V	At 80% DOD
Deep discharge voltage	2.5 V	The cells is damaged if voltage drops bellow this level
Maximal charge voltage	4 V	The cells is damaged if voltage exceeds this level
Optimal discharge current	< 20 A	0.5 C
Maximal discharge current	< 120 A	3 C, continuous for max 15 minutes from full charge
Max peak discharge current	< 400 A	10 C, maximal 5 seconds in 1 minute
Optimal charge current	< 20 A	0.5 C
Maximal charge current	< 120 A	< 3 C with battery temperature monitoring
Maximal continuous operating temperature	80 °C	The battery temperature should not increase this level during charge and discharge
Dimensions	115 x 183 x 47 mm	Millimeters (tolerance +/- 2 mm)
Weight	1.6 kg	Kilograms (tolerance +/- 150g)
Optimal torque force	12 - 15 Nm	

Characteristic curves:

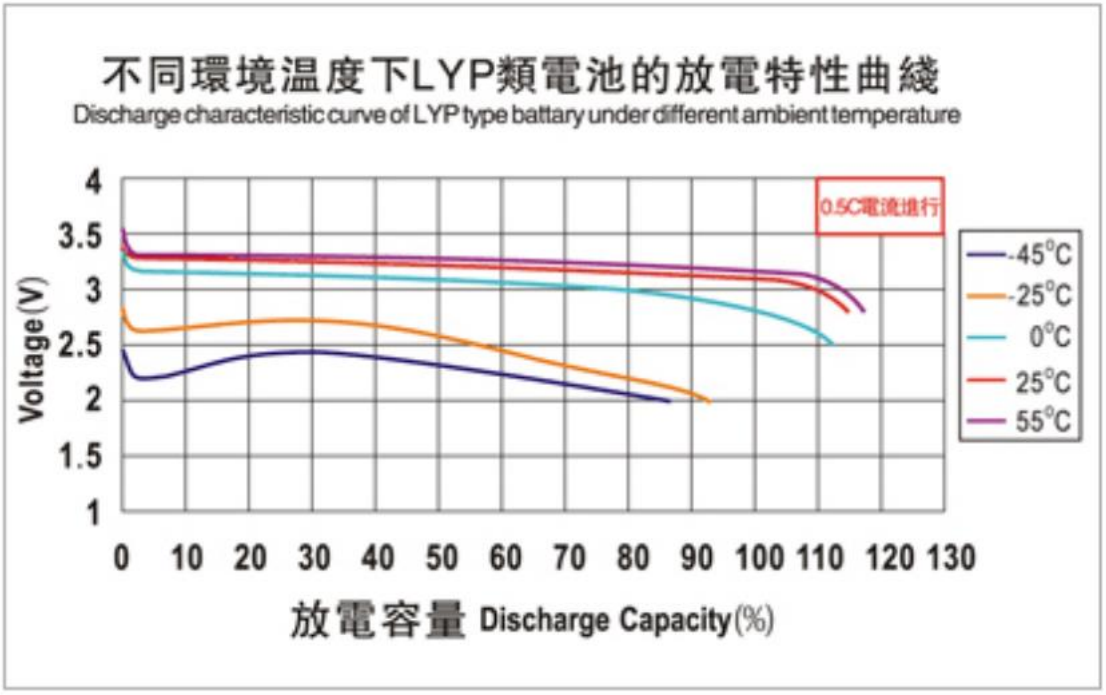

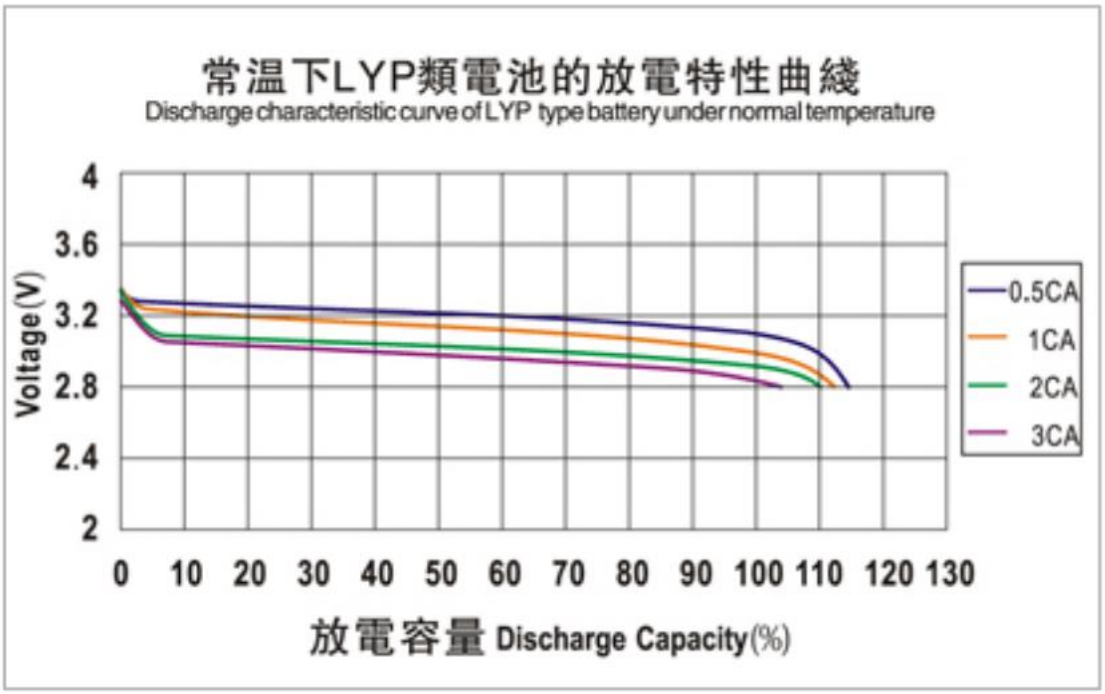
常温下LYP類電池的放電特性曲綫
Discharge characteristic curve of LYP type battery under normal temperature
Voltage(V)
4
3.6
3.2
2.8
2.4
2
0 10 20 30 40 50 60 70 80 90 100 110 120 130
放電容量 Discharge Capacity(%)
0.5CA
1CA
2CA
3CA

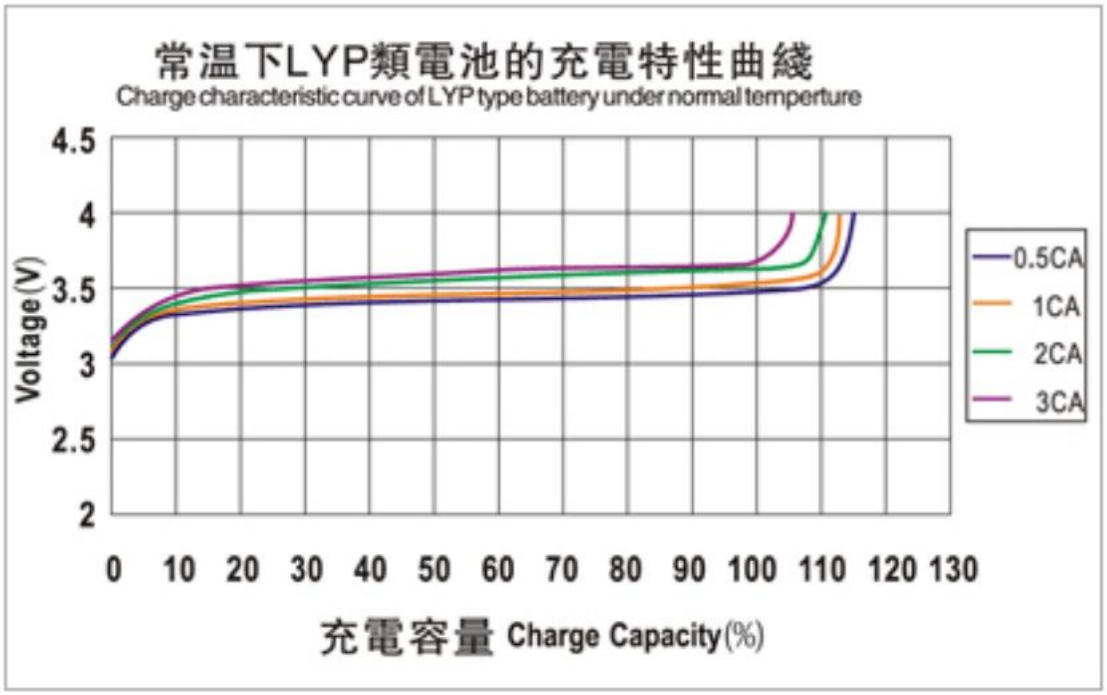
常温下LYP類電池的充電特性曲綫
Charge characteristic curve of LYP type battery under normal temperture
Voltage(V)
4.5
4
3.5
3
2.5
2
0 10 20 30 40 50 60 70 80 90 100 110 120 130
充電容量 Charge Capacity(%)
0.5CA
1CA
2CA
3CA

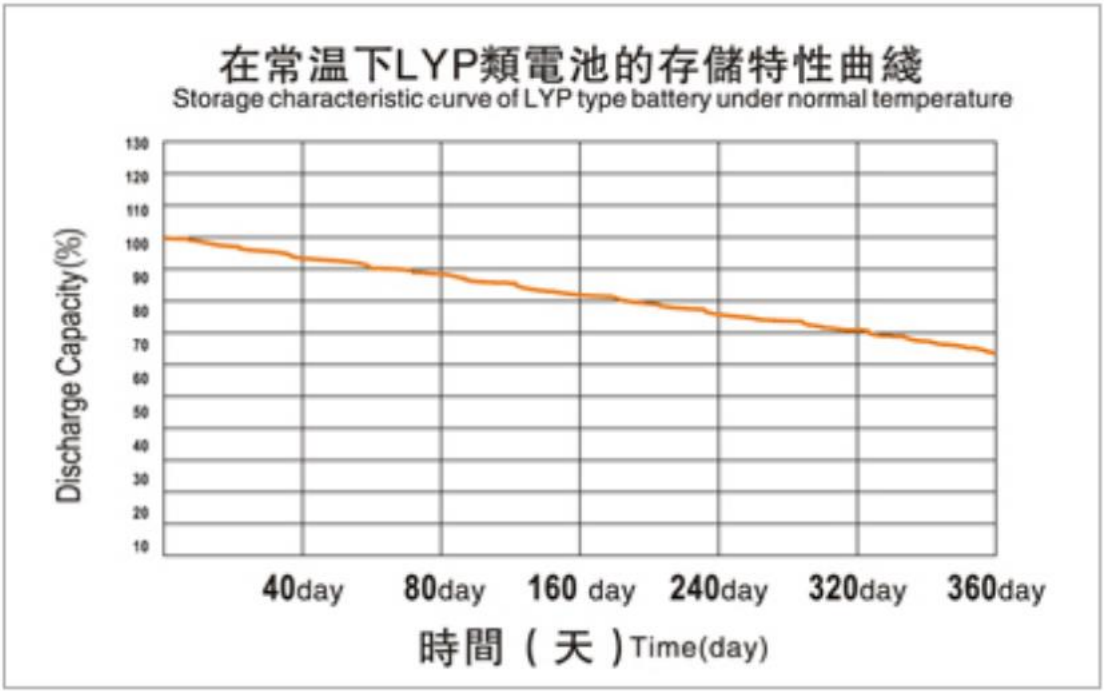
在常温下LYP類電池的存儲特性曲綫
Storage characteristic curve of LYP type battery under normal temperature
Discharge Capacity(%)
130
120
110
100
90
80
70
60
50
40
30
20
10
40day
80day
160 day
240day
320day
360day
時間（天）Time(day)

11 Apendix B – Electronic Load stability problem at low voltages

This section has an informative aim about the use of EA electronic loads like the unit used during this investigation. An issue was found during initial test trials with the setup shown in Figure 20, the issue is explained below.

In order to familiarise with the electronic load operation, initial current pulses were applied to a cell. Current values were low to start with and current values increased as confidence in the setup was gained.

When reaching currents of around 1C, the electronic load suddenly stopped working unexpectedly. This problem was reproduced several times and current traces were taken using an oscilloscope. The image below shows such behaviour:

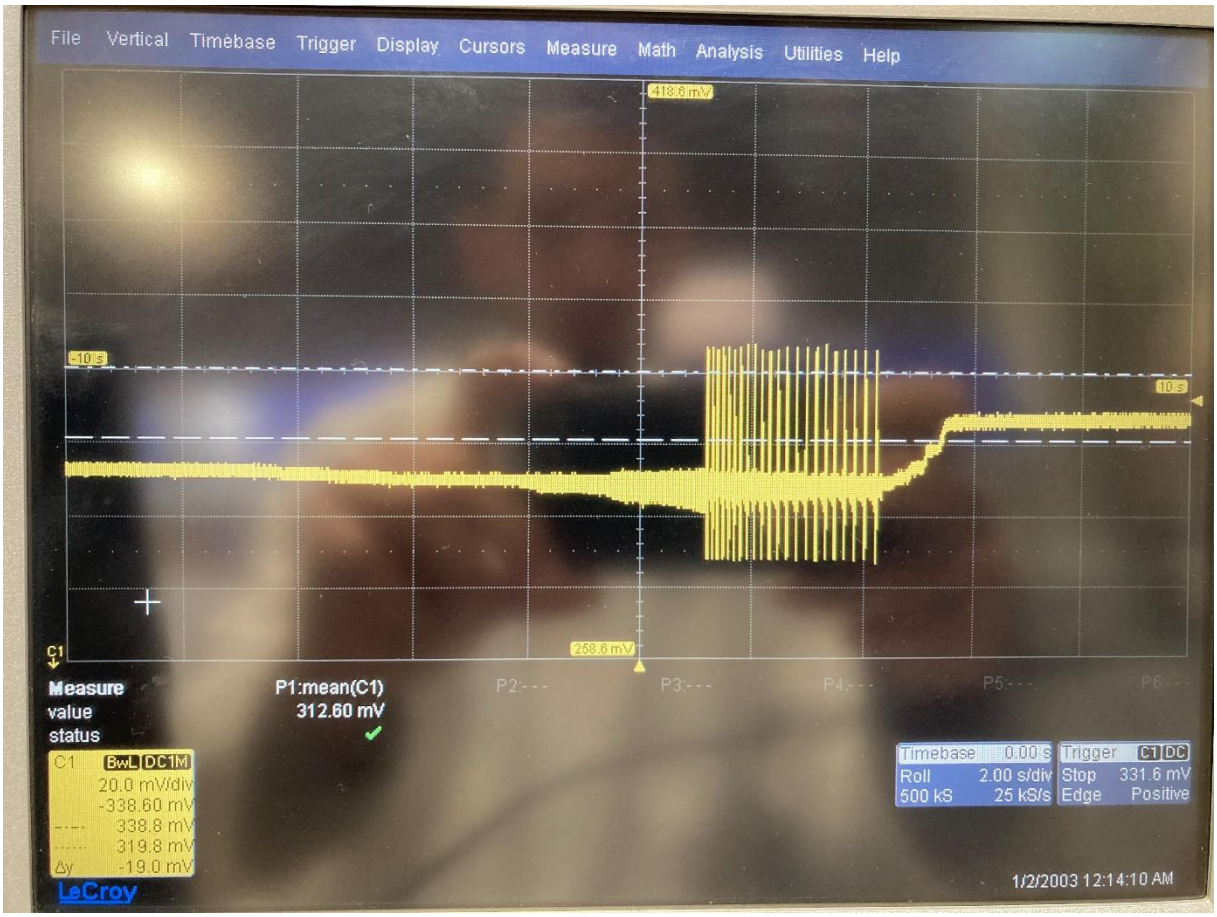

The end of the oscillatory period shows an increase in the current (from negative discharge currents to 0A), which corresponds to the deactivation of the electronic load.

Effectively, the EL's controller would not work correctly at low voltages and high currents and hence it would disable the remote-control functionality.

To solve this problem, two cells were connected in series, doubling up voltage. That was enough to avoid having this problem. This is the reason why cells were connected in series during tests.